

Notes on QSGW+DMFT algorithm

September 27, 2016

Chapter 1

The general picture

One thing that has always to be clear is the conceptual separation between lattice quantities and impurity quantities. In methods relating DMFT with other ab-initio techniques, we usually work with two Green's functions, the lattice Green's function G , which may be written in different basis and split in different components, but which is always related to the lattice framework, i.e. the real material. And the impurity Green's function \mathcal{G} which is the Green's function of an Anderson impurity model which serves as model system to solve exactly a small part of the lattice problem. A Similar distinction has to be taken in mind also for the self-energy (exchange and correlation) and for the Hartree potential.

The lattice model (DFT or GW) describes the physics of the real material. Projected or downfolded quantities are still belonging to the lattice model: they are just a local part of the full system. Even though projected, they should not be confused with quantities belonging to the impurity model. This is merely a DMFT concept and does not know anything about the lattice. They are two different worlds.

These two worlds are linked by the assumption, which is the basic assumption of DMFT, that $\Sigma_{imp} \equiv \Sigma_{loc}$. Note that *loc* will always label local lattice quantities, *imp* are impurity model quantities. Let us stress again this point: here the assumption is that there's no difference between the local part of the lattice self-energy and the self-energy of the impurity model. The point is now how to map the local part of the lattice problem onto the impurity model. This work is made by the hybridization function $\Delta(\omega)$. From the impurity perspective, it accounts for the coupling between the bath and the impurity. From the lattice perspective, it condenses the properties of the non local part of the lattice, bridging the two frameworks.

Together with the hybridization function, another important quantity that allows the mapping is the in-site effective interaction U , the Hubbard interaction which in principle can account for the renormalization of the Coulomb interaction when passing from the full lattice to the local physics. This interaction is often approximated.

Once the mapping is done, it is possible to solve the impurity model exactly through Monte Carlo methods, so that the local part of Σ^{latt} (equivalent to Σ^{imp} by hypothesis) can be computed in a more accurate way. One is happy with the method once the loop is closed, leading to the fulfilment of the self-consistency criterion $G_{loc} = \mathcal{G}$.

Chapter 2

Detailed algorithm in QSGW+DMFT

2.1 The projector

Part of Paolo's work has been to construct the projector $P_{\mathbf{k}ij}^{LL'\tau} = U_{\mathbf{k}i}^{L\tau} U_{\mathbf{k}j}^{L'\tau\dagger}$. The global index $L = l, m$ accounts for the orbital character and it takes values only for l in the coordinated subset, τ label the MT sphere. \mathbf{k} , i and j are usual momentum and band index in lattice space. This projector, constructed following Haule's prescriptions, assures causal DMFT equations (strictly negative $\text{Im}[\Sigma]$) and conserves the spectral weight of the spectral function of electrons in the correlated subset.

This does not mean, however, that other approaches, based on Wannier functions for instance, violate causality. In fact in the Wannier method the projector is by construction separable. What Rutgers' people criticise in this approaches is a less accurate treatment (or even a lost of accuracy) in the kinetic part and a less precise localization of the local quantities, which makes the use of the Anderson impurity model somewhat more questionable.

The projection operation maps the full lattice $G_{\mathbf{k}ij}(\omega)$ onto the local Green's function according to

$$\begin{aligned} G_{LL'\tau}(i\omega) &= \sum_{\mathbf{k},ij} U_{\mathbf{k}i}^{L\tau\dagger} G_{\mathbf{k}ij}(i\omega) U_{\mathbf{k}j}^{L'\tau} \\ &= \sum_{\mathbf{k},ij} U_{\mathbf{k}i}^{L\tau\dagger} [i\omega + \mu - \varepsilon_{\mathbf{k}}^0]_{ij}^{-1} U_{\mathbf{k}j}^{L'\tau}, \end{aligned} \quad (2.1)$$

where the matrix $\varepsilon_{\mathbf{k}nn'}^0 = \langle n, \mathbf{k} | H^0(\mathbf{r}, \mathbf{r}') | n', \mathbf{k} \rangle$ is the matrix element of the quasi-particle Hamiltonian $H^0(\mathbf{r}, \mathbf{r}')$, which is static and hermitian. As such, it can be split into Hartree and XC-contributions¹ $\varepsilon_{\mathbf{k}nn'}^0 = \varepsilon_{\mathbf{k}nn'}^H + \Sigma_{\mathbf{k}nn'}^0$. Note that for the moment we haven't chosen any specific basis set.

The inverse application of the projector is the "embedding" procedure, which allows one to write the local self-energy in the lattice basis. As stated above, the basic assumption of DMFT is that the local self-energy equates the impurity self-energy, that is

$$\varepsilon_{ij\mathbf{k}}^{Hloc} + \Sigma_{\mathbf{k}ij}^{loc}(\omega) = \sum_{\tau, LL'} U_{\mathbf{k}i}^{L\tau} \Sigma_{LL'\tau}^{imp}(\omega) U_{\mathbf{k}j}^{L'\tau\dagger}. \quad (2.2)$$

One has to be careful on a few aspects here. First of all, in the expression above we explicitly split the Hartree contribution from the XC-contribution in the lattice part (left

¹For the definition of Σ^0 in this context, see text below (in particular, equations (2.7), (2.8) and (2.28)).

hand side). However we included the Hartree contribution in the definition of Σ^{imp} (right hand side). Although actually confusing, this notation is somewhat in line with conventions adopted in the GW (left hand side) and DMFT (right hand side) communities. Second, the embedded $\Sigma_{\mathbf{k}ij}(\omega)$ corresponds to the local part of the fully dynamical self-energy (Hartree+XC), including vertex corrections. Hence it can not be plugged into the static QSGW self-energy as it is. Note in fact that in the left hand side, we explicitly write energy dependence on the XC self-energy. This issue can be crucial in determining the strategy to tackle the double counting problem.

Through the embedding procedure, the lattice XC self-energy is corrected to account for the local diagrams computed by the impurity solver. The resulting (full lattice) corrected self-energy is the new Σ^0 .

It is important to realize that the projection and embedding do not correspond to mere change of representation because the indexes LL' take value ONLY in the correlated subset (the space is not complete) Therefore, the combined operation of embedding and then projecting is the identity (as the starting point is a local quantity), while this is in general not true in the case of projecting and then embedding.

Making use of the projection and embedding procedure, one can write down the self-consistency condition $G_{LL'\tau}(i\omega) = \mathcal{G}_{LL'\tau}(i\omega)$

$$\begin{aligned} \sum_{\mathbf{k},ij} U_{\mathbf{k}i}^{L\tau\dagger} [i\omega + \mu - \varepsilon_{\mathbf{k}}^H - \Sigma_{\mathbf{k}}^0]_{ij}^{-1} U_{\mathbf{k}j}^{L'\tau} = \\ = [i\omega - E_{\tau}^{imp} - \Sigma_{\tau}^{imp}(\omega) - \Delta_{\tau}(\omega)]_{LL'}^{-1} . \end{aligned} \quad (2.3)$$

This relation translates in formulae the requirement that the local lattice Green's function, obtained by a projection of the full Green's function in the local space, must coincide with the impurity Green's function $\mathcal{G}_{LL'\tau}^{-1}(i\omega)$. The latter can be written as a bare impurity propagator $\mathcal{G}_{0LL'\tau}(i\omega) = [i\omega - E_{\tau}^{imp} - \Delta_{\tau}(\omega)]_{LL'}^{-1}$, plus the impurity self-energy $\Sigma_{LL'\tau}^{imp}(\omega)$.

2.2 The QSGW+DMFT algorithm step by step

In my mind the QSGW+DMFT algorithm can be summarised in the complicated flowchart of Figure 2.1. Not all steps are completely clear, and these notes have to be read as a work in progress to clarify all points. And of course, approximations can be devised to skip or fasten specific passages.

I conceptually divided the steps of the program in three groups, the QSGW steps (in blue) leading to the optimised non-local static hamiltonian describing the lattice problem. The DMFT steps (in red), concerning the mapping of the lattice problem onto the impurity model, its solution and the embedding of the impurity solution inside the lattice problem. Within the DMFT steps, the cRPA procedure (black section) accounts for the *ab-initio* determination of the in-site interaction U and its locally screened value.

The distinction in autonomous loops is not as clear as in the DFT+DMFT scheme because of the fact that the GW and the DMFT schemes are formally closer, so loops are in this context merged together to a higher degree.

1) Static (non-local) Hamiltonian: The algorithm starts from the definition of a static non-local hamiltonian $H_{ij\mathbf{k}}^0 = \langle i\mathbf{k} | H^0(\mathbf{r}, \mathbf{r}') | j\mathbf{k} \rangle$ which can be diagonalized exactly giving eigenvalues $\varepsilon_{i\mathbf{k}}^0$ and eigenfunctions $\psi_{i\mathbf{k}}^0$. This hamiltonian can come from DFT (first guess) or it can be obtained from a full QSGW calculation.

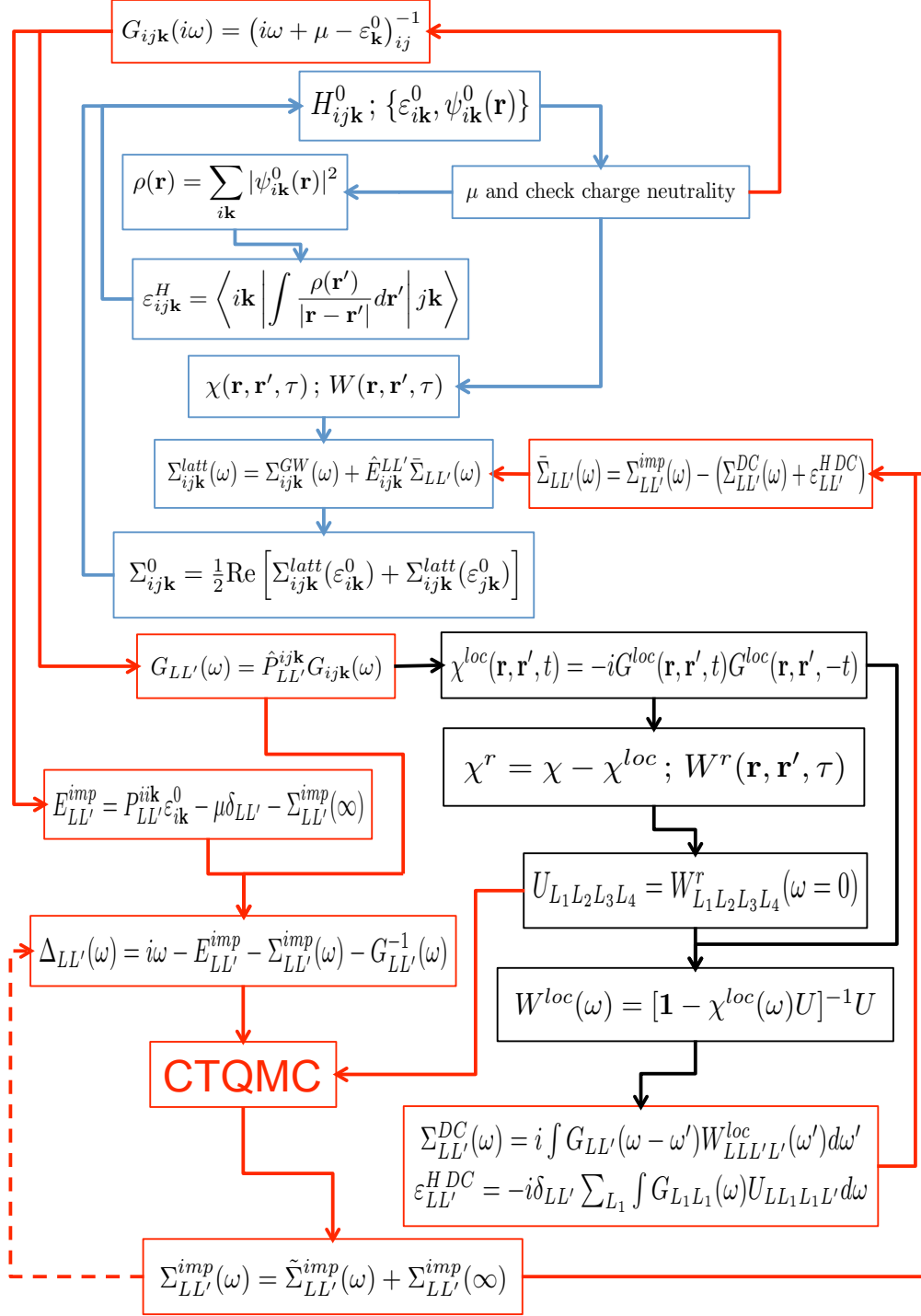


Figure 2.1: The QSGW+DMFT algorithm in its principal steps. The blue steps belong to the proper QSGW loop. Red steps concern the DMFT loop within which the black steps belong to the cRPA procedure. Sum is performed over repeated indexes in all formulas.

- 2) Chemical Potential:** From the collection of $\varepsilon_{i\mathbf{k}}^0$, one computes the chemical potential, and places correctly the Fermi energy. How this is done is mostly a technical issue, but it is a crucial step because one needs the system to be neutral in every step of the calculation.

Apparently [Haule, arxiv 2010] a good determination of μ is liable to delicate numerical instabilities that can be cured with

- i)* a plasmon-pole approximation for the self-energy and
- ii)* by subtracting and adding a fake Green's function in order to integrate numerically a smoother function on the imaginary axis.

This step becomes more important beyond the first iteration, where a distinction can be made between local and full Green's function. Then, our strategy will be probably that of adjusting the chemical potential of the local Green's function in order to match the one of the full lattice problem. Implementation details have to be clarified.

If one is happy with the lattice part, it is possible to exit here the QSGW loop (blue section in Figure 2.1) and enter the complicated DMFT loop (jump to step 9).

- 3) Density:** The density $\rho(\mathbf{r})$ of the full system is computed from the eigenfunctions $\psi_{i\mathbf{k}}^0(\mathbf{r})$ according to

$$\rho(\mathbf{r}) = \sum_{i\mathbf{k}} |\psi_{i\mathbf{k}}^0(\mathbf{r})|^2$$

This is a lattice quantity, so it is not updated within the DMFT loop.

- 4) Hartree potential:** From the density one computes the Hartree energy,

$$\varepsilon_{ij\mathbf{k}}^H = \left\langle i\mathbf{k} \left| \int \frac{\rho(\mathbf{r}')}{|\mathbf{r} - \mathbf{r}'|} d\mathbf{r}' \right| j\mathbf{k} \right\rangle. \quad (2.4)$$

- 5) Response functions:** Assuming the random phase approximation (RPA), one computes the irreducible Polarizability χ and the screened Coulomb interaction W for the lattice:

$$\chi(\mathbf{r}, \mathbf{r}', t) = -iG(\mathbf{r}, \mathbf{r}', t)G(\mathbf{r}', \mathbf{r}, -t) \quad \text{and} \quad (2.5)$$

$$W(\mathbf{r}, \mathbf{r}', t) = \int \left(\delta(\mathbf{r} - \mathbf{r}_1) - \int \frac{\chi(\mathbf{r}_2, \mathbf{r}_1, t)}{|\mathbf{r} - \mathbf{r}_2|} d\mathbf{r}_2 \right)^{-1} \frac{1}{|\mathbf{r}_1 - \mathbf{r}'|} d\mathbf{r}_1. \quad (2.6)$$

Actually, the polarizability χ is most likely computed in RPA as a sum over transitions, so relying on $\varepsilon_{i\mathbf{k}}^0$ and $\psi_{i\mathbf{k}}^0(\mathbf{r})$.

The two equations above can be performed in any basis or representation and there is no fundamental reason to prefer real space and imaginary time for doing that. As far as I understood, the way actually Sangkook performs this calculation is by Fourier transforming all quantities in real space and imaginary time.

- 6) Lattice dynamical self-energy:** The dynamical self-energy of the lattice

$$\Sigma_{ij\mathbf{k}}^{latt}(\omega) = \Sigma_{ij\mathbf{k}}^{GW}(\omega) + \sum_{LL'\tau} U_{L\tau}^{i\mathbf{k}} \bar{\Sigma}_{LL'\tau}(\omega) U_{L'\tau}^{j\mathbf{k}\dagger} \quad (2.7)$$

is computed in the GW scheme but it is corrected by the addition of $\bar{\Sigma}$. The latter term accounts for all diagrams beyond GW for the local correlated subset. This correction comes from the output of the previous DMFT calculation, so it is initialised to zero when first iterations of the QSGW algorithm are performed.

- 7) Lattice static self-energy:** Once the full-lattice dynamical self-energy is obtained, one optimizes the independent-particle problem by quasiparticlizing the self-energy

$$\Sigma_{ijk}^0 = \frac{1}{2} \text{Re} [\Sigma_{ijk}^{latt}(\varepsilon_{ik}^0) + \Sigma_{ijk}^{latt}(\varepsilon_{jk}^0)] . \quad (2.8)$$

This is not the only way to pass from a dynamical non-hermitian self-energy to a static hermitian one, however is our method of choice.

Sangkook follows a different method, relying on a linearisation of the self-energy around $\omega = 0$ but neglecting the normalization factor $Z = 1/(1 - \frac{\partial \Sigma}{\partial \omega})$ in the weight of the quasiparticle Green's function. That is just a matter of taste, however when taking static approximations (e.g., for the double counting term), one has to be careful in making coherent choices.

- 8) Close the QSGW loop:** After the quasiparticlization of the lattice self-energy, the QSGW loop can be closed by reconstructing the static hermitian non-local Hamiltonian H_{ijk}^0 and hence returning to step 1). The new Hamiltonian has an updated Hartree potential and self-energy. Steps from 1) to 8) can be performed independently from the DMFT part, so they can be repeated until convergence for fixed values (possibly null) of $\bar{\Sigma}_{LL'\tau}(\omega)$. Otherwise said, the QSGW loop updates only lattice quantities.

Before quitting the QSGW loop, it might be a good idea to recompute μ or at least to check the charge neutrality of the system. That is why the QSGW loop is quitted at step 2), after the recalculation of the new H_{ijk}^0 .

- 9) Lattice Green's function:** The starting point for beginning the DMFT loop is the calculation of the lattice Green's function. The lattice Green's function in imaginary frequency axis reads

$$G_{ijk}(i\omega) = (i\omega + \mu - \varepsilon_{ik}^0)^{-1} = (i\omega + \mu - \varepsilon_{\mathbf{k}}^H - \Sigma_{\mathbf{k}}^0)^{-1} \quad (2.9)$$

constructed by diagonalization of H_{ijk}^0 (step 1), and the updated value of the chemical potential μ (step 2).

- 10) Local Green's function:** By means of the projection operation, the local lattice Green's function is obtained

$$G_{LL'\tau}(\omega) = \sum_{ijk} U_{L\tau}^{ik\dagger} G_{ijk}(\omega) U_{L'\tau}^{jk} . \quad (2.10)$$

- 11) Impurity level:** From the high-energy expansion of the self-consistent condition (2.3), one gets the expression for the impurity level

$$E_{LL'\tau}^{imp} = \sum_{ik} U_{L\tau}^{ik\dagger} \varepsilon_{ik}^0 U_{L'\tau}^{ik} - \mu \delta_{LL'} - \Sigma_{LL'\tau}^{imp}(\infty) . \quad (2.11)$$

See chapter 5 for a derivation of the definition of the impurity level.

If it is the first DMFT iteration after a QSGW loop, $\Sigma_{LL'\tau}^{imp}(\infty)$ should be initialised to zero.

- 12) Hybridization function:** The construction of the hybridization function is justified by the self-consistent condition (2.3). Combining expressions (2.11) and (2.10) together with results from previous DMFT calculations, one computes

$$\Delta_{LL'\tau}(\omega) = i\omega - E_{LL'\tau}^{imp} - \Sigma_{LL'\tau}^{imp}(\omega) - G_{LL'\tau}^{-1}(\omega). \quad (2.12)$$

This quantity represents the coupling between the impurity and the bath. It is through the hybridization function that the mapping from the local Green's function onto the Weiss field of the Anderson impurity model is actually performed.

To construct it, one uses ingredients coming from steps 10) and 11) and from previous DMFT calculations (step 18).

- 13) Local polarizability:** We leave for a moment the DMFT loop (red path) to enter in the black section of Figure 2.1. This is the cRPA procedure, a set of definitions of other quantities required to solve the impurity problem by *ab-initio* methods, and to compute double counting contributions. In steps from 13) to 15) we will compute the (static) Hubbard interaction $U_{L_1 L_2 L_3 L_4}^r$. In step 16) we will compute the locally screened Hubbard interaction $W_{L_1 L_2 L_3 L_4}^{loc}(\omega)$.

In this step 13) one constructs the local polarizability (local bubble diagrams)

$$\chi^{loc}(\mathbf{r}, \mathbf{r}', t) = -iG^{loc}(\mathbf{r}, \mathbf{r}', t)G^{loc}(\mathbf{r}, \mathbf{r}', -t), \quad (2.13)$$

with

$$G^{loc}(\mathbf{r}, \mathbf{r}', t) = \sum_{LL'\tau} \int \mathcal{F}_{LLL'L'\tau}^\omega[G_{LL'\tau}(\omega)](\mathbf{r}, \mathbf{r}', t) d\omega \quad (2.14)$$

by means of the local Green's function (2.9) transformed in real space and imaginary time by the operator $\mathcal{F}_{LLL'L'\tau}^\omega[\cdot](\mathbf{r}, \mathbf{r}', t)$ which performs a change of representation (from LL' to \mathbf{r}, \mathbf{r}') and a Fourier transformation. Of course this operator can be split into the two distinct operations, but this is not relevant here.

As in expression (2.5), I report the polarizability in real space and imaginary time. Sangkook told me he computes them in real space and imaginary time, although there is no reason of principle to prefer this representation.

- 14) Effective interaction from the lattice:** Within the constrained RPA framework, the polarizability of the rest of the system is obtained by combining (2.5) and (2.13)

$$\chi^r(\mathbf{r}, \mathbf{r}', t) = \chi(\mathbf{r}, \mathbf{r}', t) - \chi^{loc}(\mathbf{r}, \mathbf{r}', t), \quad (2.15)$$

from which one gets the screened Coulomb interaction of the uncorrelated part of the lattice as

$$W^r(\mathbf{r}, \mathbf{r}', t) = \int \left(\delta(\mathbf{r} - \mathbf{r}_1) - \int \frac{\chi^r(\mathbf{r}_2, \mathbf{r}_1, t)}{|\mathbf{r} - \mathbf{r}_2|} d\mathbf{r}_2 \right)^{-1} \frac{1}{|\mathbf{r}_1 - \mathbf{r}'|} d\mathbf{r}_1. \quad (2.16)$$

One has to stress here that the basis where these quantities have to be computed is arbitrary, but because of equation (2.15), one needs to use the same representation for χ and χ^{loc} . As the $\{LL'\tau\}$ basis is reserved for local quantities, it looks inappropriate for χ . Similarly, the local polarizability χ^{loc} may not be well represented in the $\{ijk\}$ basis. Real space and imaginary time offer the advantage that can be a common framework for both quantities.

I'm not aware of technical difficulties that this framework would imply, as Sangkook was not clear on this point. However it seems a reasonable choice.

- 15) Hubbard interaction:** To construct the local effective interaction $U_{L_1L_2L_3L_4}^T(\omega)$ one just needs to back-transform expression (2.16) to the localised basis

$$U_{L_1L_2L_3L_4}^T(\omega) = \int \mathcal{F}_{L_1L_2L_3L_4\tau}^{\omega^{-1}} [W^r(\mathbf{r}, \mathbf{r}', t)] d\mathbf{r} d\mathbf{r}' dt \quad (2.17)$$

A possible, and very common approximation is to take the limit for $\omega \rightarrow 0$ of the expression above, hence assuming a static in-site interaction U . This is done, for example, in Rutgers' group.

Although in principle not compulsory, this approximation is assumed in most of the cases because of technical problems. In fact, one needs special quantum Monte Carlo solvers to deal with dynamical Hubbard interactions, and our solver does not do the job. Kristjan is very reluctant to implement the methods required to handle dynamical interactions. In his opinion, the possible advantages do not worth the effort to gain them.

We recently learnt from Sasha Lichtenstein that apparently the Anderson impurity model can be solved including all diagrams (for instance including spin-flip) only for static Us . Even though there are solvers able to handle dynamical Us (triqs library), not all diagrams are included in the impurity self-energy.

Assuming the static approximation, I will just omit the frequency (or time) variable

$$U_{L_1L_2L_3L_4}^T = W_{L_1L_2L_3L_4\tau}^r(\omega = 0) = \int \mathcal{F}_{L_1L_2L_3L_4\tau}^0 [W^r(\mathbf{r}, \mathbf{r}', t)] d\mathbf{r} d\mathbf{r}' dt . \quad (2.18)$$

- 16) Locally screened Hubbard:** The effective interaction (2.18) acting on the electrons of the correlated subset is screened by the local polarizability (2.13) with RPA bubbles

$$W_{LL'\tau}^{loc}(\omega) = \sum_{L_1} (\mathbf{1} - \chi_{\tau}^{loc}(\omega) U_{\tau})_{LL_1}^{-1} U_{L_1L'}^T . \quad (2.19)$$

The expression above is evaluated by Sangkook in local coordinates as I report it here. In principle all quantities above are 4-point matrices, however, because of the RPA, one can contract two indexes from the beginning, before solving the equations. The notation above and the following expressions will assume implicitly such contraction, so they are reported in the 2-point matrix form.

In the condensed expression above, $\mathbf{1} = \delta_{L_2, L_3}$, and $\chi_{\tau}^{loc}(\omega) U_{\tau}$ is a dynamical matrix expression of the kind

$$[\chi_{\tau}^{loc}(\omega) U_{\tau}]_{L_2L_3} = \sum_{L_4} \chi_{L_2L_4\tau}^{loc}(\omega) U_{L_4L_3}^T \quad (2.20)$$

where the 4-point polarizability is obtained from (2.13) by back-transforming to the local basis:

$$\chi_{L_2L_4\tau}^{loc}(\omega) = \int \mathcal{F}_{L_2L_2L_4L_4\tau}^{\omega^{-1}}[\chi^{loc}(\mathbf{r}, \mathbf{r}', t)]d\mathbf{r}d\mathbf{r}'dt. \quad (2.21)$$

All expressions above can be generalised for a dynamical Hubbard interaction. One can chose to keep time variables and perform simple products in time, or one can work in the imaginary frequency domain. In this case, a $\delta(\omega)$ has to be inserted into the definition of $\mathbf{1}$ and convolution products in frequency have to be evaluated in (2.20) and (2.19).

As far as I understood, Sangkook does follow all these steps from 13) to 16), at least at the beginning of the calculation. I think that there are other approximate ways to compute U (based on estimation of the Slater integrals F^0 , F^2 , F^4 and F^6), but I had not looked into the literature yet.

A final remark on the cRPA procedure. The whole black block should probably be done when entering the DMFT loop immediately after the QSGW, but most likely one can skip this part for every repeated iteration inside the DMFT loop.

17) The Solver: We now go back to the DMFT loop and continue from where we left it at step 12. With the (static) Hubbard interaction (2.18) and the hybridization function (2.12), one has the ingredients needed to solve the impurity problem in the Continuous Time Quantum Monte Carlo solver.

18) Impurity self-energy: The main output of the impurity solver is the impurity self-energy

$$\Sigma_{LL'\tau}^{imp}(\omega) = \tilde{\Sigma}_{LL'\tau}^{imp}(\omega) + \Sigma_{LL'\tau}^{imp}(\infty). \quad (2.22)$$

There is no fundamental reason to split between dynamical self-energy $\tilde{\Sigma}^{imp}$ and high energy tail $\Sigma^{imp}(\omega = \infty)$. However, it turns out to be very important for numerical stability to have accurate high-energy behaviour of the impurity self-energy, and also because it enters in the definition of the impurity level (2.11) and the hybridization function (2.12) As CTQMC is very noisy at high energy, interpolation schemes (splines) have to be used at this point to improve on the high-energy result of the solver. As far as I understood, for the high energy part Bismayan uses another solver, called ‘‘Hubbard 1’’, which is constructed to give a correct asymptotic result. Successively he merges the result of the two solvers by means of an interpolation scheme. This is essentially a technical issue, but disregarding a good high-energy behaviour may cause severe errors.

The asymptotic limit of the impurity self-energy is expected to be the Hartree-Fock contribution, as they are the only static diagrams. So one can either use interpolation schemes or compute Hartree-Fock contributions using the local Green’s function and the Hubbard interaction

$$\Sigma_{LL'\tau}^{imp}(\infty) = i \int G(\omega)_{LL'\tau} U_{LLL'L'}^\tau d\omega - i\delta_{LL'} \sum_{L_1} \int G_{L_1L_1\tau}(\omega) U_{LL_1L_1L'}^\tau d\omega \quad (2.23)$$

Let us stress here, that in case of a dynamical $U(\omega)$ is used, both Hartree and Fock diagrams will become energy-dependent and should both be split into high energy tail and dynamical part.

- 19) Double-counting terms:** Following the paper of Tomczak and Mark, one wants to retain all the work done by the QSGW loop, and add only local diagrams beyond GW. So one has to subtract local GW diagrams and the local Hartree contribution from $\Sigma_{LL'\tau}^{imp}(\omega)$. This consideration leads to the two double-counting terms

$$\Sigma_{LL'\tau}^{DC}(\omega) = i \int G_{LL'\tau}(\omega - \omega') W_{LLL'L'\tau}^{loc}(\omega') d\omega' = \Sigma_{LL'\tau}^{DC}(\infty) + \tilde{\Sigma}_{LL'\tau}^{DC}(\omega) \quad (2.24)$$

$$\varepsilon_{LL'\tau}^{HDC} = -i\delta_{LL'} \sum_{L_1} \int G_{L_1L_1\tau}(\omega) U_{LL_1L_1L'}^\tau d\omega \quad (2.25)$$

By definition the two terms of expression (2.23) correspond to $\Sigma_{LL'\tau}^{DC}(\infty)$ and $\varepsilon_{LL'\tau}^{HDC}$. The right hand side of equation (2.24) explicitly divides the static exchange term from the dynamical correlation term. Such a splitting can be easily put in evidence by rewriting $W^{loc} = U + U\chi U(\mathbf{1} - \chi U)^{-1} = \tilde{W}^{loc}$ (cfr. with equation (2.22)).

This is actually NOT what Sangkook is doing because he has static double-counting terms, even for the XC-contribution. He told me he sets $\omega = 0$ in equation (2.24), hence doing an approximation that apparently makes no sense. Actually this is equivalent to take static value $\Sigma^{DC}(\omega = 0)$, which is the order zero of the linearization of the self-energy he uses to construct the QSGW self-energy. So it is somewhat coherent with his quasiparticlization of the self-energy, but for us it would not be justified.

An alternative way to compute the double-counting self-energy, which would prevent one from passing through part of the cRPA steps, is

$$\Sigma_{LL'\tau}^{DC}(\omega) = i \int G_{LL'\tau}(\omega - \omega') W_{LLL'L'\tau}(\omega') d\omega' \quad (2.26)$$

$$\varepsilon_{LL'\tau}^{HDC} = -i\delta_{LL'} \sum_{L_1} \int G_{L_1L_1\tau}(\omega) U_{LL_1L_1L'}^\tau d\omega \quad (2.27)$$

where W is the full screened Coulomb interaction.

This choice can be justified by considering that, if $U(\omega)$ were taken, then $W^{loc} \equiv W$. This writing is actually inconsistent in the fact that the Hartree term is still computed with a static U . In any case, this could be a way to proceed in order to have quickly some result. The method of choice, for me, is still that of equations (2.24) and (2.25).

- 20) Corrected local self-energy and Hartree:** By subtracting both double-counting terms (2.24) and (2.25) (or alternatively (2.26) and (2.27)) from the impurity self-energy (2.22), one retains only the local diagrams beyond the GW approximation. This is the local correction to the lattice self-energy

$$\bar{\Sigma}_{LL'\tau}(\omega) = \Sigma_{LL'\tau}^{imp}(\omega) - (\Sigma_{LL'\tau}^{DC}(\omega) + \varepsilon_{LL'\tau}^{HDC}) \quad (2.28)$$

that has to be plugged into the lattice self-energy by means of the embedding procedure in expression (2.7). This correcting term includes only the local diagrams beyond the GWA.

Contextually, note that the local Hartree diagram corresponds exactly to the Hartree double counting, so no correction to the Hartree potential is needed. In practice one assumes that GW works already well for this diagram.

21) Closing the DMFT loop: To fully close the DMFT loop one has to repeat some steps of the QSGW loop. More precisely, with the new lattice self-energy (2.7) (step 6) one gets the new static self-energy (2.8) (step 7) that now embodies a better description of the local subset. So the new Hamiltonian can be diagonalised (step 1) and the new chemical potential μ (step 2) can be correctly located. Hence, the DMFT loop can be started again from its beginning (step 9) with a lattice Green's function with an enhanced impurity part.

Chapter 3

“Double-loop” or “1-shot DMFT” scheme

Yesterday me and Paolo discussed about what should be our next steps to conclude some first calculation on the QSGW+DMFT scheme. Here I try to set the main points and the strategy we would follow. I do it also in order to suggest a division of tasks.

Of course, all the steps outlined in my previous notes can not be done in a short time, so we need to look for some reasonable shortcut. The strategy could be then to do QSGW up to convergence, to use the converged lattice data to initialize the DMFT calculation and after convergence of the DMFT loop, to merge the two results. This double-loop strategy is depicted in Figure 3.1. It differs in some aspects with respect to the method devised in my previous notes, in particular in the update of the local Green’s function. This point will be developed further below.

The QSGW loop (the blue part) is performed by LM. It passes through the construction and diagonalization of a static non-local hermitian Hamiltonian, the construction of the Hartree term and the GW self-energy and the construction of the QSGW static self-energy which is static and hermitian. With the latter effective field, the new Hamiltonian is obtained and the loop can be iterated until convergence of a required quantity or group of quantities.

The DMFT loop (the red part) is composed by five blocks. The first block is the calculation (and update) of the local Green’s function and the impurity level $E_{LL'}^{imp}$ using lattice

r

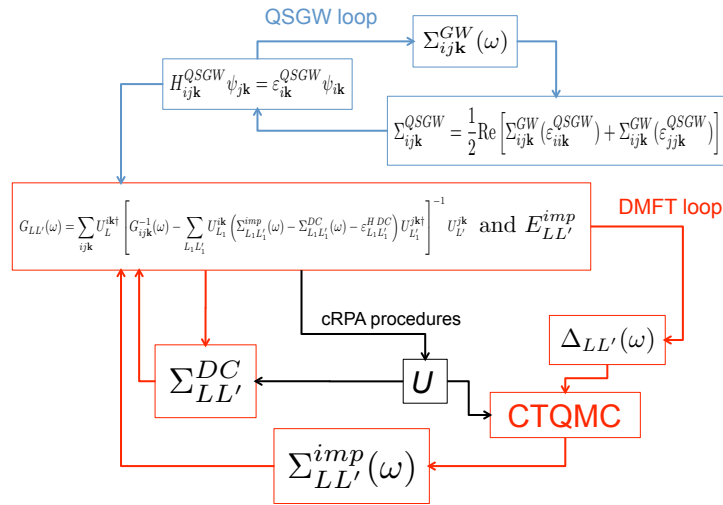


Figure 3.1: Scheme of the double loop strategy.

quantities coming from the QSGW loop and impurity quantities computed within the DMFT loop. The second step is the calculation of the hybridization function $\Delta_{LL'}(\omega)$. Together with the Hubbard interaction U , the hybridization function is fed into the CTQMC solver (third block) which returns the impurity self-energy (fourth block). In the fifth block local quantities ($G_{LL'}(\omega)$ and U) are used to construct the double counting term. Different ways to do so will be discussed below. Finally, using all the impurity quantities the updating block (the first DMFT block) is repeated and a new iteration started.

Updating $E_{LL'}^{imp}$

Within this double loop scheme, $E_{LL'}^{imp}$ is defined as

$$E_{LL'}^{imp} = \sum_{i\mathbf{k}} U_{L'}^{i\mathbf{k}\dagger} \varepsilon_{i\mathbf{k}}^{QSGW} U_{L'}^{i\mathbf{k}} - \Sigma_{LL'}^{DC}(\infty) - \varepsilon_{LL'}^{HDC} - \mu \delta_{LL'}. \quad (3.1)$$

While the QSGW eigenstates $\varepsilon_{i\mathbf{k}}^{QSGW}$ are not updated because we are outside the QSGW loop, it is important to update the chemical potential. The strategy to do that is requiring that the updated local Green's function has the same chemical potential as the QSGW Green's function.

Finally, one also includes the double counting terms at infinite energy. In principle they should be updated at each iteration of the DMFT scheme because they rely on local properties, however as a first approximation one can take initial values and keep them in every iteration. How they are computed is a complex problem that I'll address later.

TASK: *Mark, you said that you have a clear idea about how to implement the adjustment of μ . Can you do that? Do you want us to make this? In this case I think that me and Paolo we have to discuss little more with you, possibly in front of the source code, to understand where to put our hands.*

Updating $G_{LL'}(\omega)$, id est update of the self-energy

This is a delicate point. One constructs the local Green's function from the projection of the updated total Green's function. The latter includes the lattice self-energy plus corrections coming from the impurity model minus double counting terms. Currently we all agree that corrections should enter in the GW step of the QSGW loop, as depicted in my previous notes.

However, going this way would require major modifications to the code, so a different strategy is devised for the double loop procedure, closer in spirit to what me and Paolo discussed in Rutgers. In this procedure, the QSGW eigenvalues are not evaluated again so the updated Green's function G^u reads

$$\begin{aligned} G_{ij\mathbf{k}}(\omega) &= \left(\left[i\omega + \mu - \varepsilon_{i\mathbf{k}}^{QSGW} \right] \delta_{ij} - \bar{\Sigma}_{ij\mathbf{k}}(\omega) \right)^{-1} \\ &= \left(G_{i\mathbf{k}}^{-1}(\omega) \delta_{ij} - \sum_{LL'} U_L^{i\mathbf{k}} \left[\Sigma_{LL'}^{imp}(\omega) - \varepsilon_{LL'}^{HDC} - \Sigma_{LL'}^{DC}(\omega) \right] U_{L'}^{j\mathbf{k}\dagger} \right)^{-1}, \end{aligned} \quad (3.2)$$

where the definition of the correcting self-energy

$$\bar{\Sigma}_{ij\mathbf{k}}(\omega) = \sum_{LL'} U_L^{i\mathbf{k}} \left[\Sigma_{LL'}^{imp}(\omega) - \varepsilon_{LL'}^{HDC} - \Sigma_{LL'}^{DC}(\omega) \right] U_{L'}^{j\mathbf{k}\dagger} \quad (3.3)$$

has been introduced.

In expression (3.2), the lhs is the new total Green's function, while $G_{i\mathbf{k}}^{-1}$ appearing on the rhs is the old one.

QUESTION: *The $\Sigma_{LL'}^{imp}(\omega)$ provided by CTQMC is written on Matsubara frequencies, so either we write the DC term in the same frequencies, or we perform analytic continuation of $\Sigma_{LL'}^{imp}(\omega)$. Everything has to be written in the same framework. In which framework does LM work? How Matsubara's $\Sigma_{LL'}^{imp}(\omega)$ is handled at the moment?*

TASK: *The calculation of the correcting self-energy is currently handled by Paolo who is following this scheme. This procedure has to be improved though. I think that me and Paolo we could coordinate our work to improve on the way the DC terms are computed. See below.*

The double counting terms $\Sigma_{LL'}^{DC}(\omega)$ and $\varepsilon_{LL'}^{HDC}$

How to compute the double counting term is a delicate issue and many approximations are possible. Here there's a series of (more or less) justifiable approximations for the double-counting terms.

- A first very crude approximation is $\varepsilon_{LL'}^{HDC} = U(n - 1/2)\delta_{LL'}$ and $\Sigma_{LL'}^{DC}(\omega) = 0$, where U is the Hubbard interaction and n is the density of the correlated subsystem. Both are read from an external file. This is basically what the code does right now.

This is essentially an approximated Hartree term of the correlated subsystem, hence it is a static double counting term. However, it is justifiable because this is what is currently done in DFT, so it could be a good starting point. Some improvement can be achieved adding a Fock term like $\Sigma_{LL'}^{DC} = \delta_{LL'}J(n/2 - 1/2)$ or by computing $n_{LL'}$ from $G_{LL'}(\omega)$.

- A step further can be done by trying to remove from the QSGW self-energy its local part. The double counting terms hence result

$$\Sigma_{LL'}^{DC} = \sum_{i\mathbf{k}} U_L^{i\mathbf{k}} \Sigma_{i\mathbf{k}}^{QSGW} U_{L'}^{j\mathbf{k}\dagger} \quad \text{and} \quad \varepsilon_{LL'}^{HDC} = \sum_{i\mathbf{k}} U_L^{i\mathbf{k}} \varepsilon_{i\mathbf{k}}^H U_{L'}^{j\mathbf{k}\dagger} \quad (3.4)$$

This method, although more sensible than the previous one, is still not rigorous. One of its main flaws is that one loses all the advantages of working in the MBPT framework as static quantities can not be expanded in diagrams. If I remember well, Kristjan already commented this approach, right?

Both the methods above give static double counting corrections.

TASK: *I think that Paolo should focus on performing these two static approximations methods within the double-loop procedure before moving to new tasks. Could the comparison of these two methods applied to a real material be an interesting result?*

When dynamical DC terms are considered, the correct way to include them is not as formulated in the double loop strategy, but rather as displayed in the general approach,

that is including $\bar{\Sigma}_{LL'}(\omega)$ at the level of GW, and not after the quasiparticlization of the self-energy. One interesting thing would be the comparison of the two schemes (the general one and the double-loop one) with dynamical DC terms. This would require a much deeper merging of the DMFT and the QSGW loop.

Some ways to construct dynamical double counting terms might be the following.

- Using the local Green's function and U one can compute the local Hartree diagram

$$\varepsilon_{LL'}^{HDC} = -i\delta_{LL'} \sum_{L_1} \int G_{L_1L_1}(\omega) U_{LL_1L_1L'} d\omega \quad (3.5)$$

and the GW-like local diagrams

$$\Sigma_{LL'}^{DC}(\omega) = i \int G_{LL'}(\omega - \omega') W_{LLL'L'}(\omega') d\omega' \quad (3.6)$$

The way one justifies this is that if U were actually the dynamical $U(\omega) = W_r(\omega)$ as prescribed by constrained RPA, then expression (3.6) would be exact. However the approach is not coherent because the Hartree and the XC terms are not treated on the same footing since the former uses a static U , the latter implicitly assumes $U(\omega) = W_r(\omega)$.

- We agree that the most rigorous way to compute double counting terms (within the static U approximation) is what I wrote in my previous notes

$$\varepsilon_{LL'}^{HDC} = -i\delta_{LL'} \sum_{L_1} \int G_{L_1L_1}(\omega) U_{LL_1L_1L'} d\omega \quad (3.7)$$

$$\Sigma_{LL'}^{DC}(\omega) = i \int G_{LL'}(\omega - \omega') W_{LLL'L'}^{loc}(\omega') d\omega' \quad (3.8)$$

with $W^{loc} = (1 - U\chi^{loc})^{-1}U$. To compute $W_{LLL'L'}^{loc}(\omega)$ one has to implement the full cRPA scheme, which would actually allow to compute $U_{LLL'L'}$ *ab-initio* in a more correct way.

TASK: *I would focus on this dynamical DC correction part, starting from the first method, most likely implemented in the double-loop way. Then either I focus on the cRPA part in order to complete also the second method or I work on the inclusion of dynamical effects in the more general framework (correction of GW self-energy).*

Chapter 4

Projection, Embedding and Normalization

4.1 Definitions of projection and embedding

Projection The projector we use acts as follows when applied to a generic matrix A_{ijk}

$$A_{LL'} = \frac{1}{N} \sum_{ijk} U_L^{ik\dagger} A_{ijk} U_{L'}^{jk} . \quad (4.1)$$

Here the band indexes i and j run inside the energy window used to define the projection operation. Indexes L and L' are compact indexes of l, m, σ (for instance L runs from 1 to 10 if the projection is done onto a d -electron material). In matrix notation, the definition above reads $\mathbf{A}^{loc} = \hat{P}\mathbf{A}$. The sum over \mathbf{k} points is weighted, so N is the number of \mathbf{k} points in the Brillouin zone².

Embedding The operation of embedding a generic local matrix $A_{LL'}$ is defined as

$$A_{ijk} = \sum_{LL'} \hat{E}_{ijk}^{LL'} A_{LL'} = \sum_{LL'} U_L^{ik} A_{LL'} U_{L'}^{jk\dagger} . \quad (4.2)$$

In matrix notation this is written $\mathbf{A} = \hat{E}\mathbf{A}^{loc}$.

4.2 Notable properties

Products of $\mathbf{U}^{\mathbf{k}}$ have some notable properties.

Hermitian product: The product of $\mathbf{U}^{\mathbf{k}\dagger}\mathbf{U}^{\mathbf{k}}$ is Hermitian, namely:

$$O_{LL'}^{\mathbf{k}} = \sum_i U_L^{ik\dagger} U_{L'}^{ik} \text{ is Hermitian : } O_{LL'}^{\mathbf{k}} = (O_{L'L}^{\mathbf{k}})^* \quad (4.3)$$

Real sum: For each \mathbf{k}_1 , it exists a point \mathbf{k}_2 such that

$$O_{LL'}^{\mathbf{k}_2} = (O_{LL'}^{\mathbf{k}_1})^* \text{ so that } \frac{1}{N} \sum_{\mathbf{k}} O_{LL'}^{\mathbf{k}} \text{ is Real} \quad (4.4)$$

²Is summing only over \mathbf{k} -points of the irreducible Brillouin zone, an extra weight $w_{\mathbf{k}}$ would appear inside the $\sum_{\mathbf{k}}$, but it's irrelevant for our purpose.

Diagonal sum: I still can not understand how $O_{LL'}^{\mathbf{k}}$ happens to be diagonal, but this seems to be related to symmetry relations between the \mathbf{k} -points. This property is verified numerically. In this case we can impose a normalization to the transformation matrixes $U_L^{i\mathbf{k}}$ such that $\frac{1}{N} \sum_{\mathbf{k}} \mathbf{U}^{\mathbf{k}\dagger} \mathbf{U}^{\mathbf{k}} = \mathbf{1}$. Normalized projectors obey the equality

$$\frac{1}{N} \sum_{i\mathbf{k}} U_L^{i\mathbf{k}\dagger} U_{L'}^{i\mathbf{k}} = \delta_{LL'} \quad (4.5)$$

Chapter 5

The high-frequency limit

Depending on which of the two schemes one follows (the fully self-consistent one or the “1-shot DMFT”), the definition of the impurity levels $E_{LL'}^{imp}$ is different because the local Green’s function is different. In the high-frequency limit **the hybridization function vanishes by definition**, so the $E_{LL'}^{imp}$ changes to ensure that $\Delta_{LL'}(\omega \rightarrow 0) = 0$.

5.1 The limit in the full-consistent cycle

Let’s derive the expression for the impurity level $E_{LL'}^{imp}$ in the fully self-consistent scheme. We drop the site-index τ for sake of simplicity.

After N iterations of the QSGW+DMFT loop, we ask for the self-consistent relation to hold, that is we want the local part of the lattice self-energy (2.10)

$$G_{LL'}(\omega) = \sum_{i\mathbf{k}} U_L^{i\mathbf{k}\dagger} \frac{1}{i\omega + \mu - \varepsilon_{i\mathbf{k}}^0} U_{L'}^{i\mathbf{k}} \quad (5.1)$$

to coincide with the impurity self-energy

$$\mathcal{G}_{LL'}(\omega) = [i\omega - E^{imp} - \Sigma^{imp}(\omega) - \Delta(\omega)]_{LL'}^{-1} = [\mathcal{G}^{0-1}(\omega) - \Sigma^{imp}(\omega)]_{LL'}^{-1} . \quad (5.2)$$

The Green’s function (5.1), is the projection of the diagonal Green’s function $G_{i\mathbf{k}}(\omega)$. It is obtained from the eigenvalues $\varepsilon_{i\mathbf{k}}^0 = \varepsilon_{i\mathbf{k}}^H + \Sigma_{i\mathbf{k}}^0$ and the eigenstates $\psi_{i\mathbf{k}}^0(\mathbf{r})$ of the Hamiltonian $H_{ij\mathbf{k}}^0$. Note that the lattice Green’s function is diagonal on this basis. No quantity is energy-dependent as the Hamiltonian $H_{ij\mathbf{k}}^0$ is not. Because we are working in the fully self-consistent scheme, the Hamiltonian comes from the quasiparticlization of the GW self-energy corrected with the impurity self-energy minus the double counting, but it could be obtained from a hybrid calculation, Hartree-Fock or even DFT.

The impurity Green’s function $\mathcal{G}_{LL'}(\omega)$ is expressed in terms of the impurity level $E_{LL'}^{imp}$, the impurity self-energy $\Sigma_{LL'}^{imp}(\omega)$ and the hybridization function $\Delta_{LL'}(\omega)$. **All elements of $\Delta_{LL'}(\omega)$ vanish in the high-energy limit by definition of hybridization function.** In the same limit $\Sigma_{LL'}^{imp}(\omega)$ is real. For this reason, it is sensible to write $\Sigma^{imp}(\omega) = \Sigma^{imp}(\infty) + \tilde{\Sigma}^{imp}(\omega)$ with the latter matrix vanishing at $\omega = \infty$. The non-interacting impurity Green’s function is defined as $\mathcal{G}_{LL'}^0(\omega) = [i\omega - E^{imp} - \Delta(\omega)]_{LL'}^{-1}$.

Let’s take now the $\omega \rightarrow \infty$ limit of expression (5.1). Making a change of variable $z = 1/\omega$, the high-frequency limit coincides with $z \rightarrow 0^+$. For each $i\mathbf{k}$ pair, μ and $\varepsilon_{i\mathbf{k}}^0$ are constant

functions of the frequency. Let $f_{i\mathbf{k}}(z) = \frac{1}{i/z + c_{i\mathbf{k}}} = \frac{z}{i + z c_{i\mathbf{k}}}$ with $c_{i\mathbf{k}} = \mu - \varepsilon_{i\mathbf{k}}^0$, then the expansion of $f_{i\mathbf{k}}(z)$ around small positive values of z reads

$$\begin{aligned} f_{i\mathbf{k}}(z) &= f(0) + z \left. \frac{df_{i\mathbf{k}}}{dz} \right|_0 + \frac{z^2}{2} \left. \frac{d^2 f_{i\mathbf{k}}}{dz^2} \right|_0 + \mathcal{O}(z^3) \\ &\approx 0 - iz + c_{i\mathbf{k}} z^2 + \mathcal{O}(z^3). \end{aligned} \quad (5.3)$$

Using the fact that $z = 1/\omega$ and the definition of $c_{i\mathbf{k}}$, one finally gets the high-energy expansion of the local Green's function

$$G_{LL'}(\omega) \xrightarrow{\omega \rightarrow \infty} \sum_{i\mathbf{k}} U_L^{i\mathbf{k}\dagger} \left[-\frac{i}{\omega} + \frac{1}{\omega^2} (\mu - \varepsilon_{i\mathbf{k}}^0) \right] U_{L'}^{i\mathbf{k}} = -\frac{i}{\omega} \delta_{LL'} + \frac{\mu \delta_{LL'} - \sum_{i\mathbf{k}} U_L^{i\mathbf{k}\dagger} \varepsilon_{i\mathbf{k}}^0 U_{L'}^{i\mathbf{k}}}{\omega^2}, \quad (5.4)$$

where we used the fact that $\sum_{i\mathbf{k}} U_{L\tau}^{i\mathbf{k}\dagger} c U_{L'\tau}^{i\mathbf{k}} = \delta_{LL'} c$ for any complex number c .

Let's now take the same limit for the right-hand side of equation (5.2). It is less straightforward because all quantities in the expression are actually matrices, but one can make use of the exact Taylor expansion (geometric series)

$$(\mathbf{1} + \mathbf{A})^{-1} = \sum_{n=0}^{\infty} (-\mathbf{A})^n = \mathbf{1} - \mathbf{A} + \mathcal{O}(\mathbf{A}^2). \quad (5.5)$$

Let us now rewrite the impurity Green's function

$$\begin{aligned} \mathcal{G}_{LL'}(\omega) &= [i\omega - E^{imp} - \Sigma^{imp}(\omega) - \Delta(\omega)]_{LL'}^{-1} \\ &= \frac{1}{i\omega} \left[\mathbf{1} + \frac{iE^{imp}}{\omega} + \frac{i\Sigma^{imp}(\omega)}{\omega} + \frac{i\Delta(\omega)}{\omega} \right]_{LL'}^{-1}. \end{aligned} \quad (5.6)$$

Calling $\mathbf{A} = i(E^{imp} + \Sigma^{imp}(\omega) + \Delta(\omega))/\omega$, then we can expand expression (5.6) using relation (5.5). In the high energy limit, the matrix \mathbf{A} will be small enough for the expansion to be truncated at the first order. Moreover, we recall that $\Delta_{LL'}(\omega \rightarrow \infty) = 0$ and $\Sigma_{LL'}^{imp}(\omega \rightarrow 0) = \Sigma_{LL'}^{imp}(\infty)$. The resulting high energy limit, of the impurity Green's function reads

$$\mathcal{G}_{LL'}(\omega) \xrightarrow{\omega \rightarrow \infty} -\frac{i}{\omega} \delta_{LL'} - \frac{E_{LL'}^{imp} + \Sigma_{LL'}^{imp}(\infty)}{\omega^2} \quad (5.7)$$

The self-consistent condition at high energy is obtained by equating expressions (5.4) and (5.7)

$$-\frac{i}{\omega} \delta_{LL'} + \frac{\mu \delta_{LL'} - \sum_{i\mathbf{k}} U_L^{i\mathbf{k}\dagger} \varepsilon_{i\mathbf{k}}^0 U_{L'}^{i\mathbf{k}}}{\omega^2} = -\frac{i}{\omega} \delta_{LL'} - \frac{E_{LL'}^{imp} + \Sigma_{LL'}^{imp}(\infty)}{\omega^2}, \quad (5.8)$$

which leads to the definition of the impurity level

$$E_{LL'}^{imp} = \sum_{i\mathbf{k}} U_L^{i\mathbf{k}\dagger} \varepsilon_{i\mathbf{k}}^0 U_{L'}^{i\mathbf{k}} - \mu \delta_{LL'} - \Sigma_{LL'}^{imp}(\infty) \quad \text{in the fully SC scheme.} \quad (5.9)$$

The high energy tail of $\Sigma_{LL'}^{imp}(\infty)$ can be obtained by some accurate solver in this limit. For instance the ‘‘Hubbard 1’’ solver assumes that the impurity is decoupled from the bath, which corresponds to setting $\Delta_{LL'} = 0$ everywhere. Hubbard 1 is therefore more accurate the higher is the frequency we looked at. Otherwise $\Sigma_{LL'}^{imp}(\infty)$ can be computed by sophisticated interpolation schemes or by explicitly computing the Hartree-Fock terms using the impurity Green's function and local interaction U , under the assumption that these are the only diagrams contributing at high frequency.

5.2 The limit in the 1-shot DMFT

In this 1-shot DMFT scheme, the local Green's function looks like in (3.2). So, when evaluating $\mathcal{G}_{LL'} = G_{LL'}$ in the high-energy limit, new terms will appear with respect to definition (5.9).

In the 1-shot DMFT scheme

$$G_{LL'}(\omega) \xrightarrow{\omega \rightarrow \infty} \sum_{ijk} U_L^{ik\dagger} \left[\frac{1}{i\omega} \left(\delta_{ij} - \frac{\mu\delta_{ij} - \delta_{ij}\varepsilon_{ik}^{QSGW} - \bar{\Sigma}_{ijk}(\infty)}{i\omega} \right) \right] U_{L'}^{jk} \quad (5.10)$$

(compare equation (3.2)) where in the last passage the geometric series (5.5) has been truncated at the first order.

Working out all the expressions above, $G_{LL'}(\infty)$ reads

$$G_{LL'}(\infty) \approx -\frac{i}{\omega}\delta_{LL'} + \frac{\mu}{\omega^2}\delta_{LL'} - \frac{1}{\omega^2} \sum_{ik} U_L^{ik\dagger} \varepsilon_{ik}^{QSGW} U_{L'}^{ik} - \frac{1}{\omega^2} \sum_{ijk} U_L^{ik\dagger} \bar{\Sigma}_{ijk}(\infty) U_{L'}^{jk} \quad (5.11)$$

where we used the fact that $\sum_{ik} U_L^{ik\dagger} U_{L'}^{ik} = \delta_{LL'}$. We remember here that $\bar{\Sigma}$ is obtained by an embedding procedure (see equation (3.3)) reported below for ease of reference

$$\bar{\Sigma}_{ijk}(\omega) = \sum_{MM'} U_M^{ik} (\Sigma_{MM'}^{imp}(\omega) - \varepsilon_{MM'}^{HDC} - \Sigma_{MM'}^{DC}(\omega)) U_{M'}^{jk\dagger}. \quad (5.12)$$

At self-consistency, the quantity (5.11) is equal to (5.7), that is

$$\begin{aligned} -\frac{i}{\omega}\delta_{LL'} + \frac{\mu}{\omega^2}\delta_{LL'} - \frac{1}{\omega^2} \sum_{ik} U_L^{ik\dagger} \varepsilon_{ik}^{QSGW} U_{L'}^{ik} - \frac{1}{\omega^2} \sum_{ijk} U_L^{ik\dagger} \bar{\Sigma}_{ijk}(\infty) U_{L'}^{jk} &= \\ &= -\frac{i}{\omega}\delta_{LL'} - \frac{E_{LL'}^{imp} + \Sigma_{LL'}^{imp}(\infty)}{\omega^2} \end{aligned} \quad (5.13)$$

which leads to the definition of $E_{LL'}^{imp}$

$$E_{LL'}^{imp} = \sum_{ik} U_L^{ik\dagger} \varepsilon_{ik}^{QSGW} U_{L'}^{ik} + \sum_{ijk} U_L^{ik\dagger} \bar{\Sigma}_{ijk}(\infty) U_{L'}^{jk} - \Sigma_{LL'}^{imp}(\infty) - \mu\delta_{LL'} \quad (5.14)$$

The definition (5.14) is the exact definition of $E_{LL'}^{imp}$ in the 1-shot DMFT scheme.

However we can simplify it further if we can demonstrate that projecting an embedded matrix gives the same matrix, ($\hat{P} \circ \hat{E} = \mathbf{1}$). Indeed if this is the case

$$\begin{aligned} \sum_{ijk} U_L^{ik\dagger} \bar{\Sigma}_{ijk}(\infty) U_{L'}^{jk} &= \sum_{ijMM'\mathbf{k}} U_L^{ik\dagger} U_M^{ik} (\Sigma_{MM'}^{imp}(\infty) - \varepsilon_{MM'}^{HDC} - \Sigma_{MM'}^{DC}(\infty)) U_{M'}^{jk\dagger} U_{L'}^{jk} \\ &= \sum_{MM'} \delta_{LM} (\Sigma_{MM'}^{imp}(\infty) - \varepsilon_{MM'}^{HDC} - \Sigma_{MM'}^{DC}(\infty)) \delta_{M'L'} \\ &= \Sigma_{LL'}^{imp}(\infty) - \varepsilon_{LL'}^{HDC} - \Sigma_{LL'}^{DC}(\infty) \end{aligned} \quad (5.15)$$

which inserted into (5.14) gives

$$E_{LL'}^{imp} = \sum_{ik} U_L^{ik\dagger} \varepsilon_{ik}^{QSGW} U_{L'}^{ik} - \varepsilon_{LL'}^{HDC} - \Sigma_{LL'}^{DC}(\infty) - \mu\delta_{LL'} \quad \text{in the 1-shot DMFT scheme.} \quad (5.16)$$

5.3 Some comments on the properties of U

As it can be stressed by underlined statements, in both schemes we had made use of the relation

$$\sum_{i\mathbf{k}} U_L^{i\mathbf{k}\dagger} U_{L'}^{i\mathbf{k}} = \delta_{LL'} \quad (5.17)$$

which ensures the fact that the projection of a constant is a constant.

However, this is not enough in the case of the 1-shot DMFT and we definitely need that the embedding of a generic matrix $A_{MM'}$ followed by the projection gives back $A_{MM'}$. Namely we need the property

$$\sum_{ij\mathbf{k}} U_L^{i\mathbf{k}\dagger} \left(\sum_{MM'} U_M^{i\mathbf{k}} A_{MM'} U_{M'}^{j\mathbf{k}\dagger} \right) U_{L'}^{j\mathbf{k}} = A_{LL'} \quad (5.18)$$

to hold for any local matrix $A_{MM'}$. This is equivalent to require idempotency of the operator $\Pi = \hat{P} \circ \hat{E}$.

This seems to be the case for the transformations U we implemented, but I'm still puzzled how it is possible.

Chapter 6

Ensuring charge neutrality and updating the density

6.1 The Fermi-Dirac distribution

The chemical potential μ is set on the top of the valence band. For an electronic system of N electrons at equilibrium at temperature T , the number of electrons N is given by

$$N = \sum_{\mathbf{k}, i, \sigma} w_{\mathbf{k}} f_{i\mathbf{k}\sigma} \quad (6.1)$$

where $w_{\mathbf{k}}$ is the weight of the k-point \mathbf{k} and $f_{i\mathbf{k}\sigma} = (e^{\beta(E_{i\mathbf{k}\sigma} - \mu)} + 1)^{-1}$ is the Fermi-Dirac distribution at the inverse temperature $\beta = (k_B T)^{-1}$. If the calculation is not spin-polarized, then summing over all spin is equivalent to a factor 2. In this case, one gets

$$N = 2 \sum_{\mathbf{k}, i} w_{\mathbf{k}} f_{i\mathbf{k}} \quad (6.2)$$

Note that in the formulae above, the single-particle energies $E_{i\mathbf{k}\sigma}$ are supposed to be static. But this is not the case when the CTQMC local self-energy is embedded into the QSGW Hamiltonian. In this case, the Hamiltonian

$$\bar{H}_{ij\mathbf{k}}(i\omega) = \delta_{ij} \varepsilon_{i\mathbf{k}}^{QSGW} + \bar{\Sigma}_{ij\mathbf{k}}(i\omega) \quad (6.3)$$

has to be diagonalized at each energy (and each k-point)

$$\sum_j \left[\delta_{ij} \varepsilon_{i\mathbf{k}}^{QSGW} + \bar{\Sigma}_{ij\mathbf{k}}(i\omega) \right] \psi_{j\mathbf{k}}(i\omega) = \varepsilon_{i\mathbf{k}}(i\omega) \psi_{j\mathbf{k}}(i\omega) \quad (6.4)$$

and similarly for the left eigenvalue problem. The energy dependent (left) eigenvalues of $\bar{H}_{ij\mathbf{k}}(i\omega)$ are $\varepsilon_{i\mathbf{k}}(i\omega)$. To make use of equation (6.2) also in the case of energy-dependent eigenvalues, one has to write the Fermi-Dirac distribution in a different way.

Before doing so, we just remark some notable symmetry properties of the eigenvalues:

$$\text{Re}[\varepsilon_{i\mathbf{k}}(-i\omega)] = \text{Re}[\varepsilon_{i\mathbf{k}}(i\omega)] \quad : \text{ the real part is an even function,} \quad (6.5)$$

$$\text{Im}[\varepsilon_{i\mathbf{k}}(-i\omega)] = -\text{Im}[\varepsilon_{i\mathbf{k}}(i\omega)] \quad : \text{ the imaginary part is an odd function.} \quad (6.6)$$

Moreover, $\text{Re}[\varepsilon_{i\mathbf{k}}(i\omega)] > \mu$ for occupied states and $\text{Re}[\varepsilon_{i\mathbf{k}}(i\omega)] < \mu$ for empty states. It vanishes at Fermi.

By writing the Green's function in imaginary frequencies representation (Matsubara's frequencies) one can write the Fermi-Dirac distribution as

$$f_{i\mathbf{k}} = \frac{1}{\beta} \sum_{n=-\infty}^{\infty} G_{i\mathbf{k}}(i\omega_n) + \frac{1}{2} = \frac{1}{\beta} \sum_{n=-\infty}^{\infty} \frac{1}{i\omega_n + \mu - \varepsilon_{i\mathbf{k}}(i\omega_n)} + \frac{1}{2}. \quad (6.7)$$

The imaginary frequencies $i\omega_n = (2n - 1)\pi/\beta$ are the Matsubara frequencies for fermionic system and the electron number N is a real number. In fact, because of the symmetry properties (6.5) and (6.6) only the real part of the summand survives.

NOTE: As far as I understood, the actual sum over Matsubara frequencies does not converge, and one has to regularize the sum somehow. The result is the Fermi-Dirac distribution up to a constant (the 1/2 factor) that depends on the choice of the regularization. This is somewhat fuzzy to me, I haven't worked out the analytical calculation properly. However, in the low temperature limit (see below), the sum can be written as an integral and it can be performed easily. The result gives a factor 1/2. Moreover, the same factor 1/2 is found numerically: if one implements the sum over frequencies as it is, one gets the 1/2 factor numerically. In textbooks, they probably say that the sum over frequencies gives the Fermi-Dirac distribution because they make a smart choice of the regularization function, but I haven't found explicit reference to that.

NOTE: The fermionic Matsubara frequencies are equally spaced along the imaginary axis, and they form a symmetric infinite set around $i\omega = 0$. Note however that, even if the set is symmetric, frequencies are not symmetric with respect to index n : in fact they verify $\omega_{-n} = -\omega_{(n-1)}$.

This is actually due to the arbitrary choice of $n = 0$ of the definition (the $2n - 1$ factor) that makes $\omega_1 > 0$ and $\omega_0 < 0$. If one wants a symmetric set with respect to the index, it is possible to define $\omega_n = (2n - 1)\pi/\beta + \pi/\beta$ with the index $n \in \mathbb{Z} \setminus \{0\}$. Since I don't really need a symmetric index, I will not introduce this further complication.

It turns out that the numerical evaluation of expression (6.7) is not accurate even when very large frequency range is sampled. In fact, $\text{Re}[G(i\omega)]$ as a continuous function of ω has a spike at $i\omega = 0$, so a very fine frequency grid is in principle needed in the low energy range even though the $\omega = 0$ point is not in the Matsubara set. Moreover, the closer $\varepsilon_{i\mathbf{k}}(i\omega_n)$ is to μ , the sharper the spike is. This numerical problem, can be cured by subtracting and adding a Green's function $G'(i\omega_n) = (i\omega_n - \xi')^{-1}$ which has two characteristics: i) it has static energy levels ξ' and ii) the energy levels are real. In this way one gets

$$f = \frac{1}{\beta} \sum_{n=-\infty}^{\infty} (G(i\omega_n) - G'(i\omega_n)) + \left(\frac{1}{\beta} \sum_{n=-\infty}^{\infty} G'(i\omega_n) + \frac{1}{2} \right) \quad (6.8)$$

$$= \frac{1}{\beta} \sum_{n=-\infty}^{\infty} \left(\frac{1}{i\omega_n + \mu - \varepsilon(i\omega_n)} - \frac{1}{i\omega_n - \xi'} \right) + f' \quad (6.9)$$

where the band and k-point indices have been dropped for sake of simplicity.

To simplify the summation in the formula above, one can rely on the symmetry properties (6.5) and (6.6) to work only with the real part (which is an even function of the frequency).

$$f = \frac{2}{\beta} \sum_{n=0}^{\infty} \operatorname{Re} \left(\frac{1}{i\omega_n + \mu - \varepsilon(i\omega_n)} - \frac{1}{i\omega_n - \xi'} \right) + f' \quad (6.10)$$

To evaluate the latter formula in practice, a cutoff energy ω_M must be introduced so $\sum_n = \sum_{n=1}^M + \sum_{n=N+1}^{\infty}$. In order to compute the second term, one (i) takes the low-temperature limit and (ii) assumes that the eigenvalue tends to a real constant in the high energy limit. In the limit (i), $\Delta\omega = 2\pi/\beta$ tends to zero, and the Matsubara frequencies collapse forming a continuous set along the imaginary axis. Hence $\frac{2}{\beta} \sum_{n=M+1}^{\infty} = \frac{1}{\pi} \int_{\omega_M}^{\infty} d\omega$. Moreover, we make the assumption (ii) $\varepsilon(i\omega) = \operatorname{Re}[\varepsilon(i\omega_M)] = \varepsilon_M \forall \omega > \omega_M$. Under these two approximations the Fermi-Dirac distribution reads

$$f = \frac{2}{\beta} \sum_{n=1}^M \operatorname{Re} \left(\frac{1}{i\omega_n + \mu - \varepsilon(i\omega_n)} - \frac{1}{i\omega_n - \xi'} \right) + f' + \quad (6.11)$$

$$- \frac{1}{\pi} \int_{\omega_M}^{\infty} \frac{\varepsilon_M - \mu}{\omega^2 + (\varepsilon_M - \mu)^2} d\omega + \frac{1}{\pi} \int_{\omega_M}^{\infty} \frac{\xi'}{\omega^2 + \xi'^2} d\omega$$

If $\varepsilon_M - \mu$ and ξ' are not zero, then both integrals can be computed analytically:

$$\int_a^{\infty} \frac{x}{\omega^2 + x^2} d\omega = \begin{cases} \frac{\pi}{2} - \arctan(a/x) & \text{if } x > 0 \\ -\frac{\pi}{2} - \arctan(a/x) & \text{if } x < 0 \end{cases} = \arctan\left(\frac{x}{a}\right) \quad (6.12)$$

Putting all these together, one gets the expression

$$f = f' + \frac{2}{\beta} \sum_{n=1}^M \operatorname{Re} \left(\frac{1}{i\omega_n + \mu - \varepsilon(\omega_n)} - \frac{1}{i\omega_n - \xi'} \right) - \mathcal{A}(\varepsilon_M - \mu) + \mathcal{A}(\xi') \quad (6.13)$$

with the function

$$\mathcal{A}(x) = \begin{cases} \frac{1}{\pi} \arctan\left(\frac{x}{\omega_M}\right) & \text{if } x \neq 0 \\ 0 & \text{if } x = 0 \end{cases} \quad (6.14)$$

NOTE: Note that we can always make the choice $\xi' = \varepsilon_M - \mu$, that would cancel the arctan terms exactly in all cases. That would reduce the complexity of the formulas. Moreover, it seems to make the code more stable. The choice Kristjan actually did in his code is different, though. In fact he takes $\xi' = \operatorname{Re}[\varepsilon(i\omega)] - \mu$. I'm sure Kristjan already tried it, it would be interesting to know why he actually preferred the latter.

6.2 Adjusting the chemical potential

Our actual problem is that, given an hamiltonian

$$\bar{H}_{i\mathbf{j}\mathbf{k}}(i\omega_n) = \delta_{ij} \varepsilon_{i\mathbf{k}}^{QSGW} + \bar{\Sigma}_{i\mathbf{j}\mathbf{k}}(i\omega_n) \quad (6.15)$$

sampled on the Matsubara frequencies, with eigenvalues $\varepsilon_{i\mathbf{k}}(i\omega_n)$, we need to adjust the chemical potential of the system to ensure that the total number of electron N is kept

constant during the calculation. Instead of changing the chemical potential, we prefer to fix μ at the value obtained before the introduction of $\bar{\Sigma}$, and to vary instead a correcting static potential V which shifts the eigenvalues. This method also allow us to compute the density of states on the real axis (see below.)

To ensure the charge neutrality, given N^0 the reference electron number, we have to find the root of $N(V) - N^0$. This is done by the subroutine `rfalsi` called inside `getVnew`. In practice it is a refined try-and-error method, so for every V^{new} the electron number $N^{\text{new}} = N(V^{\text{new}})$ has to be computed again. Depending on the value of $N^{\text{new}} - N^0$ and dN^{new}/dV , a further step is suggested.

6.2.1 Computing $N(V)$

We can devise two ways to compute the electron number $N(V)$. In the first case we can take $\xi'_{i\mathbf{k}} = \epsilon_{i\mathbf{k}}(\omega_0) + V - \mu$ with reference to the formulas above. This is close to the method chosen by Kristijan, but in our implementation it produced some instabilities due to the \mathcal{A} functions, so I decided to make the choice $\xi'_{i\mathbf{k}} = \epsilon_{i\mathbf{k}}(\omega_M) + V - \mu$. In this case, the electron number $N(V)$ is given by

$$N(V) = \sum_{i\mathbf{k}\sigma} w_{\mathbf{k}} \left[f(\epsilon_{i\mathbf{k}\sigma}(\omega_M) + V - \mu) + \frac{2}{\beta} \sum_{n=1}^M \text{Re} \left(\frac{1}{i\omega_n + \mu - \epsilon_{i\mathbf{k}\sigma}(\omega_n) - V} - \frac{1}{i\omega_n + \mu - \epsilon_{i\mathbf{k}\sigma}(\omega_M) - V} \right) \right] \quad (6.16)$$

with no particular cases to be treated by hand.

This formula though requires the diagonalization of the Hamiltonian to be performed for the last energy before the calculation of the electron number starts. If the index n runs from 1 to M , as in the formula above, this requires two different loops on the energies, whereas with Kristijan's choice the diagonalization and the accumulation of the terms in the sum can be done at the same time. However this loss in efficiency can be overcome if the loop runs from M to 1.

6.2.2 Computing $dN(V)/dV$

One can rely once more on analytical expressions. Taking the derivative of expression (6.16) with respect to V , one gets

$$\frac{dN(V)}{dV} = \sum_{i\mathbf{k}\sigma} w_{\mathbf{k}} \left[-\frac{\beta \exp\{\beta(\epsilon_{i\mathbf{k}\sigma}(i\omega_M) + V - \mu)\}}{(1 + \exp\{\beta(\epsilon_{i\mathbf{k}\sigma}(i\omega_M) + V - \mu)\})^2} + \frac{2}{\beta} \sum_{n=1}^M \text{Re} \left(\frac{1}{(i\omega_n + \mu - \epsilon_{i\mathbf{k}\sigma}(i\omega_n) - V)^2} - \frac{1}{(i\omega_n + \mu - \epsilon_{i\mathbf{k}\sigma}(i\omega_M) - V)^2} \right) \right] \quad (6.17)$$

remembering the Fermi function $f(x) = 1/(1 + e^{x\beta})$.

Note that equation (6.17) allows for the calculation of the density of states at the real energy V . So in the same way `rfalsi` move around the value of V to ensure charge neutrality in the system, in the same way we can vary V on a grid and compute $dN(V)/dV$, getting the density of states on the real axis through quantities computed on the imaginary axis. And this can be done at every iteration of the CTQMC loop.

6.3 Updating the density

The electron density is updated following a similar way. What follows (and what has been implemented) is basically a copy of step 11 as devised in *Phys. Rev. B* **81**, 195107.

With $\bar{H}_{ijk}(i\omega_n)$ as in equation (6.3), right and left eigenfunctions read

$$\psi_{l\mathbf{k}}^R(\mathbf{r}, i\omega_n) = \sum_i C_{il\mathbf{k}}^R(i\omega_n)\psi_{i\mathbf{k}}(\mathbf{r}) \quad \text{and} \quad \psi_{l\mathbf{k}}^L(\mathbf{r}, i\omega_n) = \sum_j C_{jl\mathbf{k}}^L(i\omega_n)\psi_{j\mathbf{k}}(\mathbf{r}) \quad (6.18)$$

where they have been written as a linear combination of LDA (or QSGW) wavefunctions $\psi_{i\mathbf{k}}(\mathbf{r})$ at each energy and k-point. The index l is the index of the updated eigenstate, while the indexes i, j run over the basis of LDA or QSGW wavefunctions. Their order is the same as in the BLAS subroutine `zgeev`, which means that both $C_{\mathbf{k}}^R$ and $C_{\mathbf{k}}^L$ are matrices whose columns are the eigenvectors of \bar{H} . These matrices are such that

$$\begin{aligned} \sum_j \bar{H}_{ijk}(i\omega_n)C_{jl\mathbf{k}}^R(i\omega_n) &= \varepsilon_{l\mathbf{k}}(i\omega_n)C_{il\mathbf{k}}^R(i\omega_n) \\ \sum_i C_{il\mathbf{k}}^{L*}(i\omega_n)\bar{H}_{ijk}(i\omega_n) &= \varepsilon_{l\mathbf{k}}(i\omega_n)C_{lj\mathbf{k}}^{L*}(i\omega_n) \end{aligned} \quad (6.19)$$

The electron density can be written

$$\rho(\mathbf{r}) = \sum_{\mathbf{k}, l} \left\{ \frac{1}{\beta} \sum_{n=-\infty}^{+\infty} \psi_{l\mathbf{k}}^R(\mathbf{r}, i\omega_n) \frac{1}{i\omega_n + \mu - \varepsilon_{l\mathbf{k}}(i\omega_n)} \psi_{l\mathbf{k}}^{L*}(\mathbf{r}, i\omega_n) \right\} \quad (6.20)$$

$$= \sum_{\mathbf{k}, l} \left\{ \frac{2}{\beta} \sum_{n=1}^{+\infty} \text{Re} \left[\psi_{l\mathbf{k}}^R(\mathbf{r}, i\omega_n) \frac{1}{i\omega_n + \mu - \varepsilon_{l\mathbf{k}}(i\omega_n)} \psi_{l\mathbf{k}}^{L*}(\mathbf{r}, i\omega_n) \right] \right\} \quad (6.21)$$

$$= \sum_{\mathbf{k}} \sum_{ij} \psi_{i\mathbf{k}}(\mathbf{r}) \left\{ \sum_l \frac{2}{\beta} \sum_{n=1}^{+\infty} \text{Re} \left[\frac{C_{il\mathbf{k}}^R(i\omega_n)C_{jl\mathbf{k}}^{L*}(i\omega_n)}{i\omega_n + \mu - \varepsilon_{l\mathbf{k}}(i\omega_n)} \right] \right\} \psi_{j\mathbf{k}}^*(\mathbf{r}) \quad (6.22)$$

$$\rho(\mathbf{r}) = \sum_{\mathbf{k}} \sum_{ij} \psi_{i\mathbf{k}}(\mathbf{r}) W_{ij\mathbf{k}} \psi_{j\mathbf{k}}^*(\mathbf{r}) \quad (6.23)$$

where we introduced the density matrix $W_{ij\mathbf{k}} = \{\dots\}$. We used here the fact that the term $C_{il\mathbf{k}}^R(i\omega_n)C_{jl\mathbf{k}}^{L*}(i\omega_n)/(i\omega_n + \mu - \varepsilon_{l\mathbf{k}}(i\omega_n))$ has even real part and odd imaginary part as functions of $i\omega_n$. This has been checked numerically.

By adding and subtracting the Fermi function as done in the previous section, the matrix $W_{ij\mathbf{k}}$ is computed as

$$\begin{aligned} W_{ij\mathbf{k}} &= \sum_l \frac{2}{\beta} \sum_{n=1}^M \text{Re} \left[\frac{C_{il\mathbf{k}}^R(i\omega_n)C_{jl\mathbf{k}}^{L*}(i\omega_n)}{i\omega_n + \mu - \varepsilon_{l\mathbf{k}}(i\omega_n)} - \frac{\text{Re}[C_{il\mathbf{k}}^R(i\omega_M)C_{jl\mathbf{k}}^{L*}(i\omega_M)]}{i\omega_n + \mu - \text{Re}[\varepsilon_{l\mathbf{k}}(i\omega_M)]} \right] + \\ &+ \text{Re}[C_{il\mathbf{k}}^R(i\omega_M)C_{jl\mathbf{k}}^{L*}(i\omega_M)] f_{\beta}(\text{Re}[\varepsilon_{l\mathbf{k}}(i\omega_M)] - \mu) . \end{aligned} \quad (6.24)$$

This is done in the subroutine `cmp_denmat`. In principle the expression above should be computed summing over all Matsubara frequencies up to infinity. The truncated sum should be corrected by additional terms, but because of the $C^R(i\omega_n)C^{L*}(i\omega_n)$ factors they have not an explicit functional form as in equation (6.14). If M is high enough, I observed numerically that

$$C_{il\mathbf{k}}^R(i\omega_n)C_{jl\mathbf{k}}^{L*}(i\omega_n) \approx \text{Re}[C_{il\mathbf{k}}^R(i\omega_M)C_{jl\mathbf{k}}^{L*}(i\omega_M)] \quad \text{and} \quad \text{Im}[\varepsilon_{l\mathbf{k}}(i\omega_M)] \approx 0 . \quad (6.25)$$

These two approximations allow us to neglect the correcting term for the truncation of the Matsubara sum³.

To finally compute the updated density, one can diagonalise W and use the decomposition $W_{i\mathbf{k}} = \sum_m R_{im\mathbf{k}} w_{m\mathbf{k}} R_{mj\mathbf{k}}^{-1}$, which is performed in `diagdenmat`. One gets finally

$$\rho(\mathbf{r}) = \sum_{\mathbf{k}} \sum_m \left[\sum_i \psi_i(\mathbf{r}) R_{im\mathbf{k}} \right] w_{m\mathbf{k}} \left[\sum_j R_{mj\mathbf{k}}^{-1} \psi_j^*(\mathbf{r}) \right] \quad (6.26)$$

that should in principle allow to use usual subroutines to compute the density with rotated eigenfunctions and weighted contributions. In our case, since $W_{\mathbf{k}}$ is a symmetric real matrix (hence Hermitian), R is real (Hermitian) too. The equalities $R^{-1} = R^\dagger = R^T$ are observed to hold as expected. It can be useful to write the last expression as $\rho(\mathbf{r}) = \sum_{\mathbf{k}} \sum_m \phi_{m\mathbf{k}}(\mathbf{r}) w_{m\mathbf{k}} \phi_{m\mathbf{k}}^\dagger(\mathbf{r})$, that in matrix form reads

$$\rho_{ij} = \sum_{\mathbf{k}} \sum_m \phi_{im\mathbf{k}} w_{m\mathbf{k}} \phi_{mj\mathbf{k}}^* \quad (6.27)$$

because in the code the function $\phi_{m\mathbf{k}}(\mathbf{r})$ is actually expressed as a matrix of coefficient $\Phi_{im\mathbf{k}}$ where the index i runs over the LDA (or QSGW) eigenstates. The weights $w_{m\mathbf{k}}$ and the matrices $\Phi_{im\mathbf{k}}$ are computed by `mkdmftstates` and passed to the subroutine `addrbl` devoted to the calculation of the electronic density.

³I think that in equation (6.20) there should appear somewhere a factor 1/2 as in the previous section but I can't figure out where. In expression (6.24), which is similar to the one reported in the PRB paper, this factor does not appear presumably because it's cancelled by the second term in the Matsubara sum, analogously to what done in the previous section. However the presence of the terms $C^R C^{L*}$ complicates the things in the same way as for the correcting terms discussed above. I assume the two approximations discussed above still apply.

Chapter 7

Maximum Entropy Method (MEM)

These notes are a rearrangement of the information I found in

1. J. E. Gubernatis, M. Jarrel, R. N. Silver and D. S. Sivia, *Phys. Rev. B* **44**, 6011 (1991)
2. Johan Schött's Master Thesis in Applied Physics, *Chalmers University of Technology*, Gothenburg (2013)
3. The `maxent_run.py` code by K.Haule.

The terminology I use in these notes might be uncorrect or misleading. The main goal of these notes is to understand how to use the `maxent_run.py` code and, in case, to rewrite it.

7.1 An inverse problem

After the CTQMC run, the updated lattice Green's function $G_{ijk}(i\omega)$ can be computed on the Matsubara frequency axis. However if we want to extract from the theoretical data a spectral function $A(\omega)$ or an other quantity to be compared with some experimental data, then we have to be able to write the Green's function on the real axis. This is actually a non-trivial inverse problem of the kind

$$G(i\tau) = \int_{-\infty}^{+\infty} K(\omega, i\tau)A(\omega)d\omega \quad (7.1)$$

where $G(i\tau)$ is the computed Green's function in imaginary time, periodic in $0 \leq \tau \leq \beta$, $K(\omega, i\tau)$ is a known Kernel and $A(\omega)$ is the desired spectral function on the real axis. The inverse temperature $\beta = (k_B T)^{-1}$ where k_B is the Boltzman constant. Band and k-point indexes have been dropped for simplicity.

The Kernel is actually known and it comes from the fluctuation-dissipation theorem. For a fermionic Green's function⁴ it reads

$$K(\omega, i\tau) = \frac{e^{-\tau\omega}}{1 + e^{-\beta\omega}} \quad (7.2)$$

Despite the known form of the Kernel, the inversion problem is highly non-trivial and non-univoque slutions can be found. In solving the problem then, one solution among all possible ones has to be picked, but with what criteria shall we chose? We might have some prior

⁴The “+” sign in the denominator accounts for the Fermi statistics, it would be a “-” in case of bosonig Green's function (like phonons).

knowledge about sum rules, normalization, asymptotic behaviour, or other properties that might allow us to restrict the set of possible candidates. But how can we incorporate this prior information in a quantitative way?

In the maximum entropy method (MEM), this question is reformulated in terms of a statistical inference problem: “*What is the most probable spectral function that produces the theoretical Green’s function and how confident are we in the answer?*”. To identify what is the most probable $\hat{A}(\omega)$ spectral function, an information entropy measure is associated to several trial spectral functions; the one which maximizes the information entropy is the most probable one. To reformulate equation (7.1) in a statistical language and to invert the problem via quantities that can be calculated, the theory relies on the Bayes’ theorem.

7.2 Bayes’ theorem and statistical approach

It has been shown⁵ that any inference problem can be restated in a statistical language. In our case, what we want to maximize is the probability density functional $P[A|\bar{G}, I]$, that is the probability of having a spectral function A , given the CTQMC Green’s function \bar{G} and the prior information I . According to the Bayes’ theorem we can write

$$P[A|\bar{G}, I] \propto P[\bar{G}|A, I]P[A|I] \quad (7.3)$$

The conditional probability of measuring A , given \bar{G} and I is proportional to the conditional probability of measuring \bar{G} , given A and I times the conditional probability of measuring A given I . The lhs is also called “a-posteriori PDF”.

The first term in the rhs of expression (7.3) is called “likelihood function” and it is a measure of how probable is to obtain the computed Green’s function \bar{G} from a given spectral function A and prior information I . The second term is called “entropic prior PDF”, and can be seen as a weight that measures how compatible is the spectral function A with our prior information about it.

The strong point of the MEM method seems to me this: the inverse problem in the lhs of (7.3), is reformulated in terms of a direct problem that can be easily computed (the likelihood function) and a weight. Our aim being to maximize the lhs, we will try to maximize the product of the two terms of the rhs by means of a statistical sampling of the two probability distributions.

7.2.1 The likelihood function

How do we compute the likelihood function $P[\bar{G}|A, I]$?

Imagine you have a trial spectral function $A(\omega)$, then you can compute the corresponding Green’s function $G(i\tau)$ through equation (7.1). The distance between this trial Green’s function $G(i\tau)$ and the QMC Green’s function $\bar{G}(i\tau)$ can be used to estimate the probability of getting \bar{G} from A .

To do so, we need to define a measure between Green’s functions and the error associated to any of the discretized measures $G(i\tau_j)$ (note the discretization of the time) This is actually simple within the assumption that data are independent and they are subject to Gaussian

⁵R. T. Cox *Am. J. Phys* **14**,1 (1946)

noise with width $\sigma_j = \sigma(\tau_j)$. Under these hypothesis, one can write the likelihood PDF as

$$P[\bar{G}|A, I] = \frac{e^{-\chi^2/2}}{\prod_j \sqrt{2\pi\sigma_j^2}} \quad \text{with} \quad \chi^2 = \sum_j \frac{[\bar{G}(i\tau_j) - G(i\tau_j)]^2}{\sigma_j^2} \quad (7.4)$$

Maximizing $P[\bar{G}|A, I]$ corresponds then in a minimization of the least-squares distance χ^2 between the actual \bar{G} and the trial G .

7.2.2 The entropic prior

What information do we have about the spectral function A ? We can state for sure that it is an additive, non-negative function. For this information, there are arguments⁶ leading to the entropic form

$$P[A|I, m, \alpha] = \frac{e^{\alpha S[A, m]}}{Z_S(\alpha)} \quad \text{with} \quad S[A, m] = \int \left[A(\omega) - m(\omega) - A(\omega) \ln \left(\frac{A(\omega)}{m(\omega)} \right) \right] d\omega \quad (7.5)$$

This is the conditional probability of measuring A , given the prior informatio I , the model m and α . The model $m(\omega)$ is actually the function that allows us to incorporate all information we have in a quantitative way. If there were no data, the ‘‘a-posteriori’’ probability would coincide with the entropic prior which is maximised when $A(\omega) = m(\omega)$, that’s where the name maximum entropy comes from. The parameter α can be seen as a controlling parameter, establishing the relative importance of the entropic prior and the likelihood function (see below).

7.2.3 A functional minimization problem

Putting together equations (7.4) and (7.5) into equation (7.3), it turns out that

$$P[A|\bar{G}, I] \propto \exp \left\{ \alpha S[A, m] - \frac{\chi^2}{2} \right\} . \quad (7.6)$$

The argument of the exponential function has to be maximized, that corresponds in minimizing the functional

$$Q[A](\alpha) = \frac{\chi^2}{2} - \alpha S[A] . \quad (7.7)$$

Note that the parameter α can be seen in this context as a mixing parameter that controls how important is the entropic prior in the sum. If $\alpha \rightarrow 0$, the a-posteriori PDF coincides with the likelihood function, that is no prior information is included in the conditional probbability. Conversely, it $\alpha \rightarrow \infty$, then we rely completely on the prior information and the maximization will be attained for $A(\omega) = m(\omega)$. The functional Q has to be minimized both to respect to $A(\omega)$ and α .

⁶see for instance E. T. Jaynes, in *Maximum entropy and Bayesian Methods* edited by J. H. Justice (Cambridge University Press, Cambridge, England 1986); S. F. Gull, in *Maximum Entropy and Bayesian Methods in Science and Engineering* edited by G. J. Erickson and C. R. Smith (Kluwer Academic, Dordrecht, 1988); D. S. Sivia, *Los Alamos Sci.* **19**, 180 (1990) and references therein; J. Skilling, in *Maximum entropy and Bayesian Methods* edited by J. Skilling (Kluwer Academic, Dordrecht, 1989) and S. F. Gull *ibid.*

At fixed α , the minimization with respect to $A(\omega)$ is done in *maxent_run.py* by means of a Metropolis algorithm. In practice several trial spectral functions $A'(\omega) = A(\omega) + \delta A(\omega)$ are generated and the changes $\delta A(\omega)$ with respect to the previous $A(\omega)$ are accepted or rejected depending on the changes is $Q[A] - Q[A']$. This leads to an improvement on the image $A_\alpha(\omega)$ based on statistical sampling. See below for more details.

Once a reliable $A_\alpha(\omega)$ is found, one can minimize $Q[A_\alpha](\alpha)$ with respect to α . It is possible to show⁷ that this minimization procedure leads to the equation

$$\frac{-2\alpha S}{\text{Tr}\{\Lambda(\Lambda + \alpha)^{-1}\}} = 1 \quad (7.8)$$

where we introduced

$$\Lambda_{ij} = \sqrt{A(\omega_i)} \frac{\sum_{\tau} K(\omega_i, \tau) K(\omega_j, \tau)}{\sigma^2(\tau)} \sqrt{A(\omega_j)} \sqrt{d\omega_i d\omega_j} \quad (7.9)$$

The value of α is then updated depending on ratio (7.8) and the calculation of a new spectral function $A(\omega)$ is repeated until convergence.

7.3 Actual implementation maxent_run.py

The python script *maxent_run.py* manipulates the CTQMC self-energy to get the imaginary-time Green's function and manipulates the output spectral-function $\hat{A}(\omega)$ of the maximum entropy method to get the Green's function and the self-energy in the real frequency axis. The actual maximum entropy method on $\bar{G}(i\tau)$ is implemented in two modules: *maxentropy.py* and a collection of fortran routines *maxent_routines.f90*.

The general picture of the method is a three step procedure:

Sample Green's function: From the CTQMC self-energy $\Sigma(i\omega)$ one constructs the Green's function in imaginary time $\bar{G}(i\tau)$ with $0 \leq \tau \leq \beta$ by Fourier-transform the Matsubara Green's function $G(i\omega) = 1/(i\omega - \Sigma(i\omega))$.

Maximum entropy method: The maximum entropy method is applied to $\bar{G}(i\tau)$ in order to reconstruct the most probable spectral function on the real frequency axis $\hat{A}(\omega)$.

The real-frequency Self-energy: Applying the Kramers-Kronig relations to the spectral function $\hat{A}(\omega)$, the most probable real-frequency Green's function $\hat{G}(\omega)$ and the corresponding self-energy are obtained as $\hat{\Sigma}(\omega) = \omega - 1/\hat{G}(\omega)$.

The core of the procedure is of course the Maximum Entropy method that is performed by *maxentropy.py*.

7.3.1 Maximum entropy method in maxentropy.py

After the calculation of the Green's function on the imaginary time, the python function *MaximumEntropy* is called. The actual implementation relies basically on two loops: an

⁷The proof actually rely on the minimization of the second order term in a Taylor expansion of $Q[A](\alpha)$, but going through the details of such demonstration is beyond the purpose of these note. See Appendix of reference [1].

outer loop to get best estimate of $\hat{\alpha}$ (number of iterations controlled by input variable `Nitt`), an inner loop to get the best estimate of \hat{A} (annealing loop, controlled by variable `Asteps`). The implementation scheme follows several steps.

1. A frequency mesh ω_j is defined in the real frequency axis (non necessarily uniform). The corresponding array $d\omega_j$ to be used in integration is also defined.
2. The integration kernel $K(\omega_j, i\tau)$ is computed according to formula (7.2). Because of the discretization of the time variable, $K_{j\tau}$ is actually a matrix of dimensions $(2Nw+1) \times Nt$.
3. The Gaussian weight $\mathbf{sxt} = 1/\sigma_\tau^2$ appearing in formula (7.4) is computed for all imaginary times (note the discretized-time notation). It can be uniform ($\sigma_\tau = \sigma$, input `idg=1`) or proportional to the Green's function ($\sigma_\tau = \sigma\bar{G}_\tau$, input `idg=0`). The value of σ is defined by the input variable `deltag`.
4. The model $m_i = m(\omega_i)$ is constructed. It can be a flat distribution (input `iflat=0`), a gaussian distribution (input `iflat=1`) with variance σ , or it can be imported from a file "model.dat" (input `iflat=2`).
5. Create a random spectral function $A_i = A(\omega_i)$.
6. Compute the matrix $T_{ij} = [\sum_\tau K_{i\tau}K_{j\tau}/\sigma_\tau^2](d\omega_i d\omega_j)^{-1}$ which is the part of Λ_{ij} that does not depend on A_i , so its construction can be left outside the loops.
7. **Outer loop starts for a maximum of `Nitt` iterations** Within this loop one improves on the estimate of α by evaluating the ratio (7.8)
 - 7.1. Some initialisation before the inner loop is started. The most notable quantity here is da_i , a vector added to A_i used to improve on the prediction
 - 7.2. **Inner loop starts for `Asteps` iterations** Within this loop one improves on the estimate of A_i using the Metropolis algorithm.
 - 7.2.1. Compute the Green's function $G_\tau = \sum_i A_i K_{i\tau}$.
 - 7.2.2. Compute $\chi^2 = \sum_\tau (\bar{G}_\tau - G_\tau)^2 / \sigma_\tau^2$ as in equation (7.4).
 - 7.2.3. For all real frequencies, a trial A'_i is generated and the corresponding G'_τ and $\chi^{2'}$ are computed. The difference $Q - Q'$ is evaluated and the changes to the spectral function are accepted according to the Metropolis algorithm. That is if $Q' < Q$ the trial spectral function is accepted and becomes the new one, if $Q' \geq Q$ then changes are accepted with a probability proportional to $\exp\{Q - Q'\}$.
 - 7.2.4. A method to adjust automatically the internal parameters of the Metropolis algorithm based on the acceptance/trial ratio is implemented.

The annealing loop ends here
- 7.3. After the annealing loop, the improved spectral function A_i for the given α is used to compute the entropic value $S = -\sum_i A_i \ln(A_i/m_i) d\omega_i$
- 7.4. The matrix $C = \Lambda(\Lambda - \alpha)^{-1}$ is computed and its trace $\text{Tr}C$ evaluated (see equations (7.8) and (7.9)).

7.5. The ratio (7.8) is evaluated. If it is close to 1 within the tolerance parameter `min_ratio` the outer loop is exited, otherwise α is improved by increasing or decreasing it of a random amount.

The outer loop ends here

8. **Broadening loop starts for `Nr` iterations** Within this loop, the procedure of the outer loop is repeated with two main differences. First: at the beginning of each loop, the spectral function is broadened by a convolution with a Gaussian. Second: no update of α is performed even though the ratio (7.8) is evaluated. It is worthy to note that in Kristjian's test, this loop is skipped as `Nr=0` (probably not necessary).

9. The final best estimate of the spectral function is recorded in the file "dos.out".

7.3.2 Input and Output files

The program `maxent_run.py` requires two input files: the CTQMC self-energy (argument of `maxent_run.py`) and the parameters file `maxent_params.dat` of which here is a template:

```
params={'statistics': 'fermi', # fermi/bose
        'Ntau'      : 300,    # Number of time points
        'L'        : 10.0,   # cutoff frequency on real axis
        'Nw'       : 400,    # number of frequency points on real axis
        'gwidth'   : 2*10.0, # width of gaussian
        'idg'      : 1,      # Gaussian error. 1:s=deltag ; 0:s=deltag*Gt
        'deltag'   : 0.01,   # error
        'Asteps'   : 4000,   # anealing steps
        'alpha0'   : 1000,   # starting alpha
        'min_ratio' : 0.005,  # condition to finish, what should be the ratio
        'iflat'    : 1,      # model. 0:constant ; 1:Gaussian s=gwidth ; 2:model.dat
        'Nitt'     : 1000,   # maximum number of outside iterations
        'Nr'       : 0,      # number of smoothing runs
        'bwth'     : 0.03,   # smoothing width
        'Nf'       : 40,     # inverse Fourier:high-freq limit from the last Nf points
        }
```

The maximum entropy procedure is applied to $\bar{G}(i\tau)$ for all channels of the input self-energy. During the runtime, several files are produced, some of them are temporary files.

Spectral function: For each step `itt` of the outer loop (and for each step of the broadening loop), the spectral function of the current channel is recorded on files `dos_itt` (and `dos_Nitt`). As these files are overwritten, only the last channel is left at the end of the run. The final real-frequency spectral function of channel `c` is recorded in file `dos.out.c`. At each channel `c`, the temporary file `dos.out` with the spectral function $A(\omega)$ is written and copied into `dos.out.c` and `dosn`. The latter is another temporary file used as input of the Kramers-Kronig.

Green's function: The output of the Kramers-Kronig transformation for channel `c` is recorded in `Gc`. At channel `c`, files `gt0.c` and `gtn.c` report respectively the initial (\bar{G}) and final (G) imaginary-time Green's function. The latter is a copy of the temporary file `gtn` overwritten at each channel.

Self-energy: The real-frequency self-energy extracted from `Gc` is recorded in `sig.c` for the channel `c`. These data are then all collected in the main output file `Sig.out` where the resulting self-energy on the real-frequency axis is recorded. First column is the frequency, followed by real and imaginary parts of the self-energy per channel `c`.

During the runtime, the status of the calculation is printed on the screen. It's curious to note that redirecting the output to a file (like a log file) shuffle the order of the lines.

7.4 Results

In this section I would like to present some application of the method. I tried to apply the method do Ni and LSCO, but the parameters I've chosen are not good, and spectra are meaningless. I report in any case a test calculation from Kristjan's folder. Unfortunately I don't know where the input self-energy comes from, so the calculation has to be taken just as a reference of what "reliable" results should look like.

7.4.1 Kristjan's input self-energy

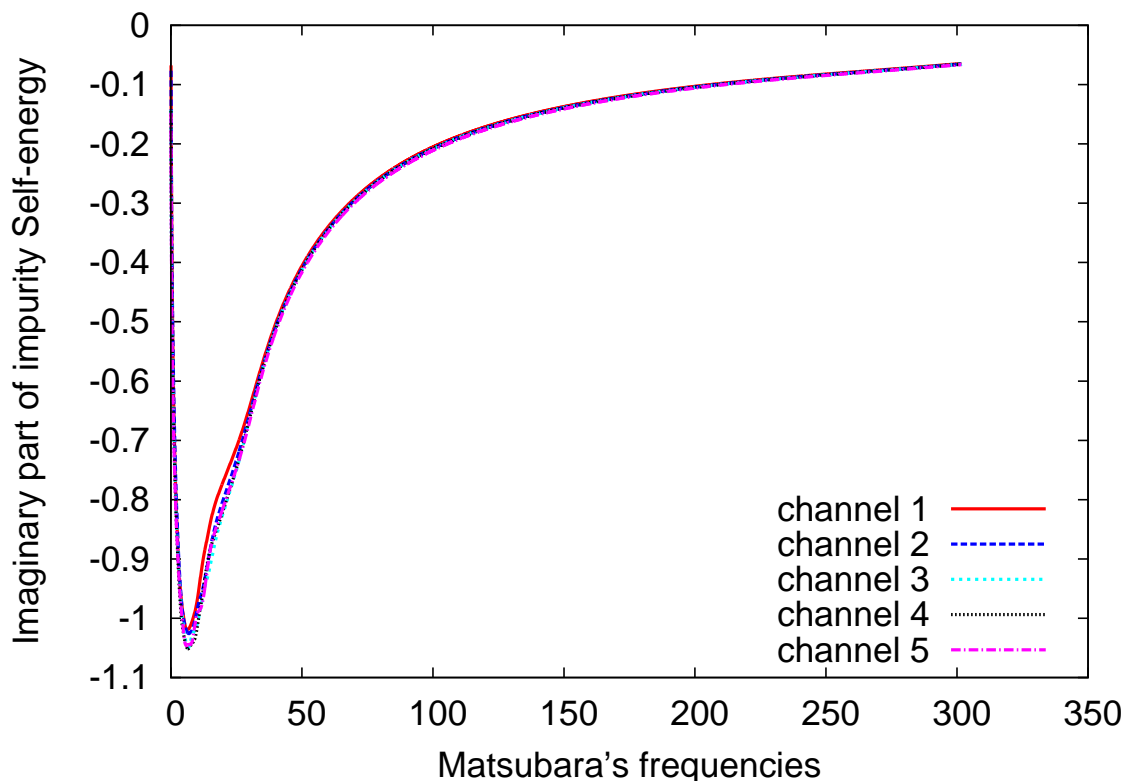


Figure 7.1: Imaginary part of the impurity self-energy on the Matsubara's frequency axis.

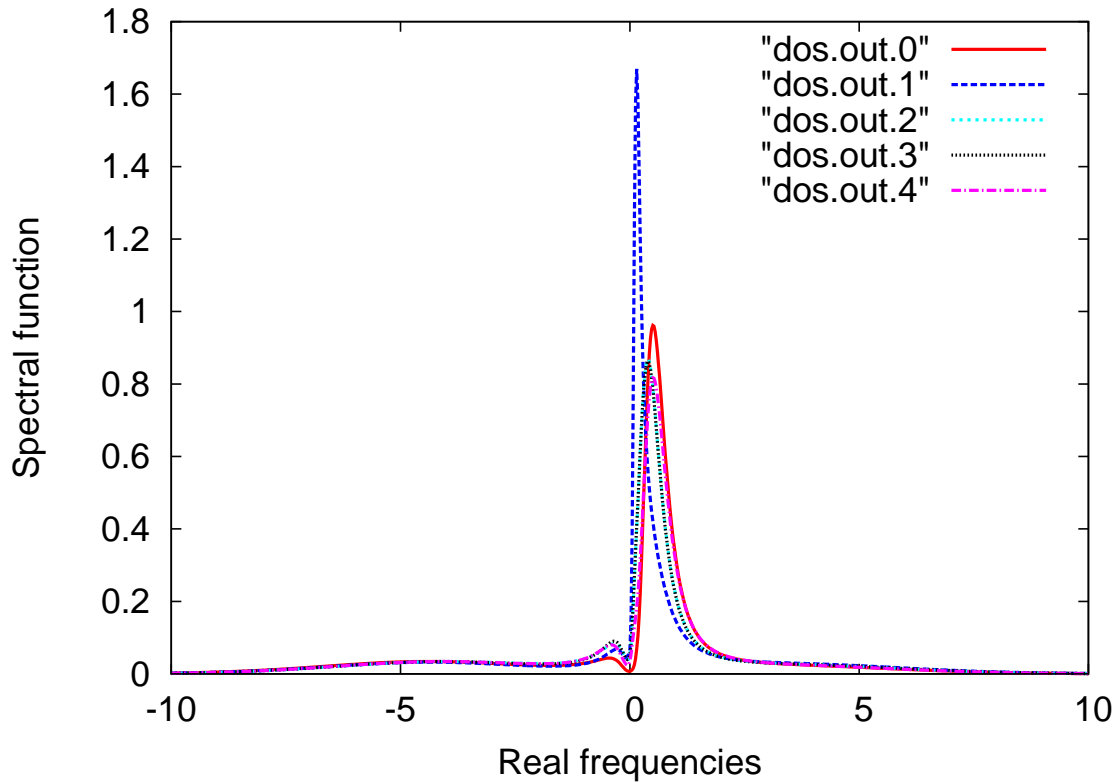


Figure 7.2: Spectral function resulting from the self-energy of Figure 7.1.

In this test case, the impurity is a d -level system. The original calculation is not spin-polarized so the resulting self-energy has only five channels. In Figure 7.1 I report the imaginary part of the self-energy on the imaginary-frequency axis.

The input file used to execute the maximum entropy method is the *maxent_params.dat* reported at the beginning of section 7.3.2. The resulting spectral function is reported in Figure 7.2.

Chapter 8

Dynamical Double-counting (I) : cRPA or cLDA?

In order to get a dynamical $\Sigma_{LL'}^{DC}(\omega)$ from a static in-site interaction U , one has to downfold high-energy excitations (and non-local effects) in a proper way into U . This chapter is devoted to this aspect. There are two methods to get U from *ab-initio* calculations, the constrained LDA method and the constrained RPA.

8.1 The interaction U in d - and f -electron elements

In the work by D. van del Marel and G. A. Sawatzky [Phys. Rev. B **37**, 10674 (1988)], it is given an expression for the effective Hubbard U interaction on d and f electrons for atoms in a metallic matrix. In particular the expression is given for the local Coulomb repulsion

$$F_l^0 = \frac{1}{2l+1} \sum_{m<n} \int \int |\psi_{lm}(\mathbf{r}_1)|^2 \frac{1}{|r_1 - r_2|} |\psi_{ln}(\mathbf{r}_2)|^2 d\mathbf{r}_1 d\mathbf{r}_2 \quad (8.1)$$

for $l = 2$ or 3 (d or f electrons) and $\psi_{lm}(\mathbf{r})$ single-particle wave functions in the same shell (identical principal quantum number). The local exchange between two electrons in the same shell is given by

$$J_l = \frac{1}{2l+1} \sum_{m<n} \int \int \left[\psi_{lm}(\mathbf{r}_1) \psi_{ln}(\mathbf{r}_1) \frac{1}{|r_1 - r_2|} \psi_{lm}(\mathbf{r}_2) \psi_{ln}(\mathbf{r}_2) \right] d\mathbf{r}_1 d\mathbf{r}_2 \quad (8.2)$$

which is actually a combination of Slater integrals F^2 , F^4 (and F^6 in case of f electrons). More specifically $J = (F^2 + F^4)/14$ for $l = 2$ and $J = (286F^2 + 195F^4 + 250F^6)/6435$ for $l = 3$.

The additional integral C is also given

$$C_{l=2} = \frac{1}{14} \left(\frac{9}{7} F^2 - \frac{5}{7} F^4 \right) \quad C_{l=3} = \frac{1}{6435} \left(286 F^2 + \frac{780}{11} F^4 - \frac{1750}{11} F^6 \right) \quad (8.3)$$

which account for the multipole contributions due to the nonspherical charge distribution in cases when the shell is neither full or at half-filling.

Further on in the paper, the authors provide the effective Hubbard U in terms of F^0, J and C , together with empirical linear expressions to evaluate them.

Table 8.1: Local interaction terms (in eV)

	La ($Z = 57; 4f^1$)	Cu ($Z = 29; 3d^9$)
F^0	6.7	3.18
J	0.69	1.19
C	0.3105	0.6069

Following their prescriptions, the parameters for La and Cu are both $U_2 = F^0 - J - C$, where the empirical expressions for the coefficients are given in Table 8.1. I'm pretty sure about Cu, but for La the paper is not so clear, as it is the first in the $4f$ row, but it prefers to occupy the $5d$ shell.

The U used in Sangkook's calculations [arXiv 1504.07569] is for the Cu $3d^1$ shell. It is $F^0 = 12$ eV and $J = 1.4$ eV. The value of F^0 is particularly high with respect to what obtained by the empirical formula of van der Marel and Sawatzky. This may be due to the fact that in their work, they provide values for atoms embedded into a metallic environment. Metallic screening can be the reason why the density-density interaction F^0 so low than what used by Sangkook.

8.2 Overview on the cLDA method to compute U

In constrained LDA (cLDA), the basic idea is to obtain the effective interaction acting on d (or f) electrons from derivatives of the total energy. The main equation is

$$\frac{\partial \varepsilon_i}{\partial n_j} = \langle ij | (v + f_{xc}) \epsilon^{-1} | ij \rangle \approx \langle ij | W | ij \rangle \quad (8.4)$$

where ε_i is the energy of the level i and n_j is the occupation number of the level j . The RPA approximation is used to make f_{xc} disappear from the equation above.

The basic idea is to compute the change in energy (usually taken as the center of mass of the band of the d states) with respect to the change of occupancy of the d band. In order to do that, one has to constraint the number of occupancy and perform several calculations by changing the constraint. Furthermore, the hopping between d states and the rest of the system is suppressed.

This method actually has some deficiency in treating the screening from the non-correlated orbitals [see F. Aryasetiawan, K. Karlsson, O. Jepsen and U. Schönberger, Phys. Rev. B **74**, 125106 (2006)]. Moreover, in Mark's code there is not ready-made way to constraint the occupancy of a given level, so it would require new tools to be implemented.

8.3 Overview on the cRPA method to compute U

The idea behind the constrained RPA is to compute the effective interaction on the d (or f) by splitting the one-electron transitions into those between levels of the correlated subset and the rest. The basic assumption is that

$$\chi^0(\tau) = \chi_d^0(\tau) + \chi_r^0(\tau) \quad (8.5)$$

where the correlated polarizability $\chi_d^0(\tau)$ is computed as a sum over all transitions where both initial and final states are in the correlated subset. The full screened interaction W is defined in RPA as

$$W^{-1}(\tau) = v^{-1} + \chi^0(\tau) = v^{-1} + \chi_d^0(\tau) + \chi_r^0(\tau) \quad (8.6)$$

that is the Coulomb interaction v screened by all independent-particle transitions of the system.

The effective interaction $U(\tau)$, is defined as the bare interaction v screened by the rest of the system

$$U^{-1}(\tau) = v^{-1} + \chi_r^0(\tau) . \quad (8.7)$$

The full screening is finally recovered once the effective interaction is screened by the correlated transitions

$$W^{-1}(\tau) = U^{-1}(\tau) + \chi_d^0(\tau) . \quad (8.8)$$

It is worth noting that in cRPA the effective $U(\tau)$ depends on time, so it is dynamical because $\chi_d^0(\tau)$ is. What is usually done is to take the static limit and use $U = U(\omega = 0)$, but this can be justified only if $U(\omega)$ is almost constant in the energy region of interest. This can be the case if we are interested in the low-energy physics (around Fermi) and the window to split between correlated and non-correlated transitions is big enough. However, once a static U is taken, the full screening of equation (8.8) is not obtained anymore. Instead one finds the approximated screening

$$W_{\text{loc}}^{-1}(\tau) = U^{-1} + \chi_d^0(\tau) . \quad (8.9)$$

where the subscript ‘loc’ has been used to use the same notation of Sangkook and following the notation of equation (2.19).

For cRPA see also steps from 13 to 16 in chapter 2.2.

8.4 Comments